

Exploring and Analyzing the Systemic Delivery Barriers for Nanoparticles

Lin Wang, Skyler Quine, Alex N. Frickenstein, Michael Lee, Wen Yang, Vinit M. Sheth, Margaret D. Bourlon, Yuxin He, Shanxin Lyu, Lucila Garcia-Contreras, Yan D. Zhao, and Stefan Wilhelm*

Most nanomedicines require efficient *in vivo* delivery to elicit meaningful diagnostic and therapeutic effects. However, en route to their intended tissues, systemically administered nanoparticles often encounter delivery barriers. To describe these barriers, the term “nanoparticle blood removal pathways” (NBRP) is proposed, which summarizes the interactions between nanoparticles and the body’s various cell-dependent and cell-independent blood clearance mechanisms. Nanoparticle design and biological modulation strategies are reviewed to mitigate nanoparticle-NBRP interactions. As these interactions affect nanoparticle delivery, the preclinical literature from 2011–2021 is studied, and the nanoparticle blood circulation and organ biodistribution data are analyzed. The findings reveal that nanoparticle surface chemistry affects the *in vivo* behavior more than other nanoparticle design parameters. Combinatory biological-PEG surface modification improves the blood area under the curve by $\approx 418\%$, with a decrease in liver accumulation of up to 47%. A greater understanding of nanoparticle-NBRP interactions and associated delivery trends will provide new nanoparticle design and biological modulation strategies for safer, more effective, and more efficient nanomedicines.

1. Introduction

Nanoparticles are used in medicine as carriers for diagnostic and therapeutic agents due to their uniquely tunable physicochemical properties, including size, shape, stiffness, surface chemistry (so-called 4S parameters), material composition, and their capacity for loading with contrast agents and drugs.^[1] However, it is a key challenge in nanomedicine to efficiently deliver systemically administered nanoparticles to diseased tissues and cells in the body.^[2] For example, a meta-analysis of preclinical studies found that only 0.7% (median) of systemically administered nanoparticles reach solid tumor tissues.^[3] Additionally, up to 99% of systemically administered nanoparticles may accumulate in the liver (Figure 1a).^[4] These delivery challenges contribute to the limited clinical translation of certain nanomedicines, such as cancer nanomedicines.^[5,6]

Efficient and effective systemic nanoparticle delivery to malignant tissues and

organs, such as tumors, is a complex challenge because nanoparticles face numerous barriers upon entering the body.^[7] These barriers include: i) nanoparticle-protein interactions in the blood leading to opsonization (Figure 1b) and nanoparticle interactions with organs and cells of the Mononuclear Phagocyte (MPS) or Reticuloendothelial (RES) Systems (Figure 1c), which result in rapid blood clearance and undesired distribution in healthy organs; ii) endothelium in the target organ, restricting the underlying cells from interacting with the nanoparticles in the bloodstream; iii) dense extracellular matrix and high interstitial fluid pressure in the abnormal tumor microenvironment, preventing deep tissue penetration of nanoparticles; iv) inefficient cellular internalization, which limits the effectiveness of intracellular therapeutic interventions; v) endosomal entrapment and lysosomal degradation, which impact the transport of the therapeutics to the appropriate intracellular organelles. Several informative review papers have summarized and discussed some of these barriers.^[8–10]

This article comprehensively explores and discusses cell and organ functions that enable nanoparticle clearance from blood circulation.^[11] In Section 2, we introduce the proposed

L. Wang, S. Quine, A. N. Frickenstein, M. Lee, W. Yang, V. M. Sheth, Y. He, S. Lyu, S. Wilhelm


Stephenson School of Biomedical Engineering
University of Oklahoma
Norman, OK 73019, USA
E-mail: stefan.wilhelm@ou.edu

M. D. Bourlon, L. Garcia-Contreras
College of Pharmacy
University of Oklahoma Health Sciences Center
Oklahoma City, OK 73117, USA

Y. D. Zhao
Department of Biostatistics and Epidemiology
University of Oklahoma Health Sciences Center
Oklahoma City, OK 73012, USA

Y. D. Zhao, S. Wilhelm
Stephenson Cancer Center
Oklahoma City, OK 73104, USA

S. Wilhelm
Institute for Biomedical Engineering, Science, and Technology (IBEST)
Norman, OK 73019, USA

 The ORCID identification number(s) for the author(s) of this article can be found under <https://doi.org/10.1002/adfm.202308446>

DOI: 10.1002/adfm.202308446

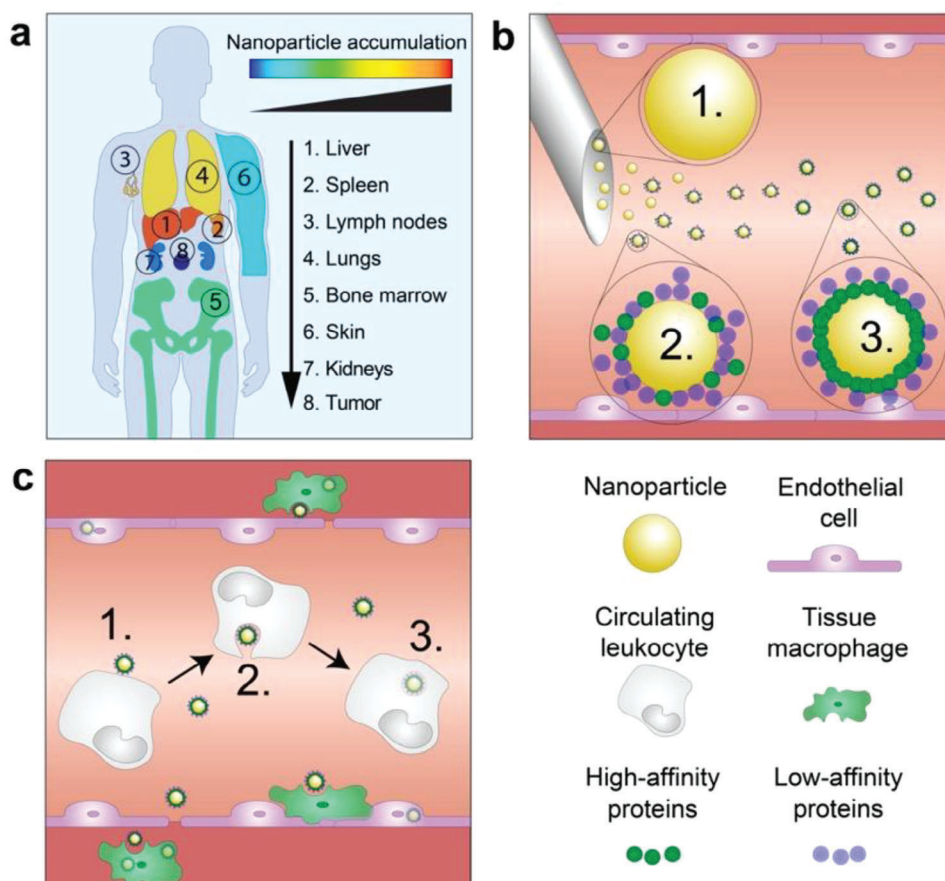


Figure 1. Examples of nanoparticle delivery barriers. a) The body's biological and physical barriers affect nanoparticle biodistribution. Note: Depicted relative biodistribution and nanoparticle accumulation may vary significantly for different nanoparticle formulations and doses. b) Upon intravenous administration 1), nanoparticles are exposed to blood components. This exposure changes the nanoparticle's synthetic identity to a biological identity. During the initial exposure phase 2), proteins with varying binding affinities interact dynamically with the nanoparticle surface. Over time 3), a hard protein corona forms around the nanoparticle surface composed of proteins exhibiting relatively high binding affinity and low exchange rate. Proteins with less affinity and high exchange rate interact with the hard corona and create a dynamic soft corona. c) Cells of the nanoparticle blood removal pathways (NBRP), including tissue-resident macrophages, circulating leukocytes, and various endothelial cell types, uptake circulating nanoparticles from the blood by various mechanisms.

terminology “nanoparticle blood removal pathways (NBRP)”. This terminology aims to address and overcome the limitations associated with the MPS/RES terms in nanomedicine. In the subsequent section, we discuss the NBRPs in detail, highlighting the phagocytic and anatomical characteristics of various relevant organs. To overcome rapid blood clearance of nanoparticles and improve target organ delivery, researchers explored and applied two main strategies over the past few decades: i) the modulation of nanoparticle design; and ii) the modulation or pre-treatment of the body's biological environment. Therefore, in the subsequent Sections 4 and 5, we review how nanoparticle physicochemical properties and biological modulation affect nanoparticle-NBRP interaction, respectively. In Section 6, we present a comprehensive survey of the published preclinical literature from 2011–2021. Through this analysis, we systematically evaluate the status of nanoparticle design strategies and statistically analyze how the nanoparticles' physicochemical properties affect nanoparticle-NBRP interactions. Based on this

literature analysis, we discuss key insights and strategies for the nanomedicine field.

2. Definition of the Nanoparticle Blood Removal Pathways (NBRP)

Compared with traditional small molecule drugs, nanoparticles experience a different journey after systemic administration partially due to their increased size.^[12,13] Small molecule drugs, especially ones that are <900 Daltons and that exhibit high permeability, mainly undergo non-specific translocation from the blood to the body's tissues by diffusion and other processes through the membranes of various cell types.^[14,15] However, the continuous endothelium along most blood vessels becomes a barrier for nanoparticles, minimizing translocation and accumulation in organs.^[16] To cross this barrier, nanoparticles need to traverse endothelial cells through transcytosis and/or other mechanisms.^[13] The major factors deciding where and how the nanoparticles

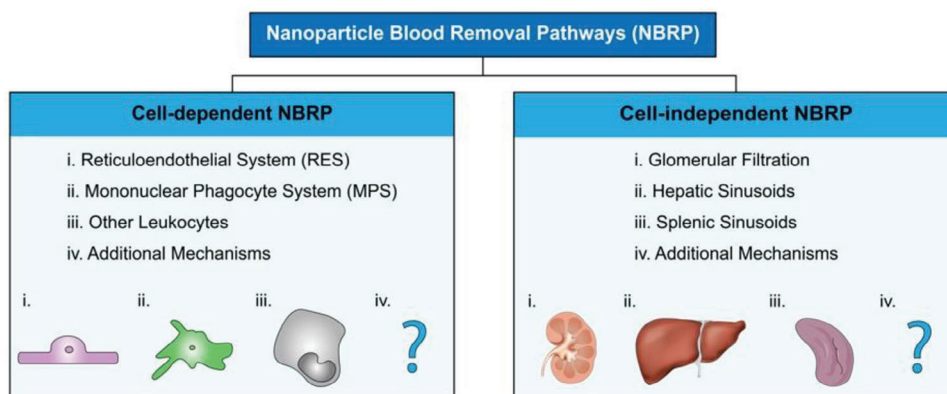


Figure 2. Schematic overview of the Nanoparticle Blood Removal Pathways (NBRP). The NBRP is a broadly defined term that summarizes multiple mechanisms of nanoparticle clearance and sequestration. The two main branches of the NBRP are the cell-dependent and the cell-independent NBRP. The cell-dependent NBRP include traditional systems used to describe nanoparticle clearance, such as the MPS and RES, and further incorporates other cell-mediated pathways, such as clearance by other leukocytes and additional unknown/undiscovered pathways and mechanisms. The cell-independent NBRP include physical clearance mechanisms, such as glomerular filtration in the kidneys and the sinusoids of the liver and spleen. As additional mechanisms of nanoparticle clearance may be discovered in the future, these mechanisms will be adequately described by the proposed NBRP terminology.

are removed from the blood circulation include the endothelium morphological features (e.g., fenestrae, and vessel continuity and integrity), organ physiological characteristics, and the profile and location of phagocytic cells within each organ.^[17] While each of these pathways is recognized to contribute individually to removing nanoparticles from blood circulation, the terminology that comprehensively summarizes these multifaceted mechanisms and their combined effects is lacking in the nanomedicine field.

The MPS and RES are terms widely used in the nanomedicine field to refer to cells that pose biological barriers to nanoparticle delivery. Although the MPS and RES are relevant for nanoparticle clearance and sequestration, the literature references these terms inconsistently.^[18–23] Chronologically, the term “RES” was first used in 1924 to describe any cell that accumulated systemically administered vital stains (i.e., dyes that stain living tissues), which were thought to be endothelial cells.^[24] The term “MPS” was introduced in 1972 as a replacement when it was discovered that many of the cells involved in clearing macromolecules and foreign particulates from the blood were monocytes or originated from bone marrow.^[25,26] Subsequent research revealed that, in addition to monocytes, true endothelial cell types actively clear particulates from the blood,^[27] including scavenger endothelial cells (SECs)^[28] and liver sinusoidal endothelial cells (LSECs).^[22,29,30]

The MPS term categorizes three ontologically and functionally distinct cell types that endocytose nanoparticles as “mononuclear phagocytes”: i) monocytes; ii) macrophages; and iii) dendritic cells.^[31,32] In addition to these cells, the RES term encompasses various endothelial cell types that exhibit endocytic behaviors. Yet, MPS and RES categories leave out certain cell types, including leukocytes, such as B cells and T-cells, capable of internalizing nanoparticles.^[33,34] Further, MPS and RES systems rely on endocytic nanoparticle sequestration mechanisms, leaving out important physical nanoparticle clearance and sequestration mechanisms, such as glomerular filtration. These mechanisms, other than MPS and RES, warrant continued studies, given their critical role in removing nanoparticles from the blood and subsequently impeding nanoparticle delivery.

To consolidate and expand the MPS/RES terminologies in the nanomedicine field, we propose the term “Nanoparticle Blood Removal Pathways” (NBRP) as a more practical and comprehensive expression to describe organs, cells, and other mechanisms that directly contribute to removing nanoparticles from the blood (Figure 2).

Cell-mediated NBRP include the MPS, RES, and other cellular mechanisms of nanoparticle sequestration and clearance. Cell-independent NBRP include physical mechanisms, such as glomerular filtration in the kidneys and the unique blood flow profile of the liver and spleen. Additional mechanisms of nanoparticle clearance will likely be discovered in the future. We defined the NBRP terminology broadly so that any future nanoparticle blood clearance mechanisms can be adequately categorized. The term “clearance” is used in this manuscript to describe the removal of nanoparticles from the blood.

3. NBRP Organs, Cells, and Clearance Pathways

We describe the interactions between nanoparticles and the NBRP for different organs and tissues. For each organ, we discuss three main components affecting nanoparticle clearance: i) the blood-endothelium interface; ii) phagocytic cells; and iii) tissue anatomical characteristics.

3.1. Blood

When nanoparticles enter the bloodstream, they immediately encounter a complex biological environment.^[10,35,36] Within this environment, nanoparticles transition from their lab-designed “synthetic identity” to their physiologically-determined “biological identity” (Figure 1b). Plasma proteins form what is known as a “protein corona” around nanoparticles, partially blocking their interactions with target cells and increasing non-specific interactions.^[37,38]

The protein corona has been suggested to have a multilayered structure, with the composition and organization

of the integrated proteins affecting the ultimate fate of the nanoparticle.^[37,39] Opsonins are any type of blood serum component that can facilitate phagocytic recognition. Among these components, antibodies and complement proteins like C3, C4, and C5 are widely recognized.^[40] The process by which opsonins bind to foreign particles is termed opsonization. The inclusion of opsonins in the protein corona can mark a nanoparticle for phagocytosis by circulating leukocytes or tissue-resident macrophages.^[41] This process can occur through the alternative, classical, and lectin pathways of the complement cascade, a bloodborne sector of the immune system that protects the body from foreign pathogens and particles.^[42–44] Nanoparticle uptake can also occur through other types of endocytosis, including clathrin-dependent endocytosis, caveolae-mediated endocytosis, clathrin and caveolin-independent endocytosis, and macropinocytosis. The various mechanisms of nanoparticle cellular internalization have been reviewed in greater detail elsewhere.^[45,46]

Nanoparticles may interact with any blood component: biomolecules, such as serum proteins, sugars, nucleic acids, lipids, and cells, including red blood cells (RBCs), white blood cells, and endothelial cells.^[47–49] All of these interactions are highly dependent on nanoparticle design. It has been reported that nanoparticles could further interact with RBCs in different ways: i) the lysis of RBCs (hemolysis),^[50] ii) the entry into RBCs,^[51] and iii) the adsorption to the RBC membrane.^[52–55] However, many of these studies were performed *ex vivo*, which does not fully capture the biological and physical complexities of the *in vivo* environment. Therefore, further research is encouraged to better probe and understand the *in vivo* interactions between nanoparticles and RBCs.

Besides mediating protein corona formation and opsonization, which promotes uptake in various NBRP, the blood itself can function as an NBRP by sequestering nanoparticles into various circulating cells. A study by Yang et al. reported a time-dependent distribution of 500-nm polystyrene nanoparticles in blood cells. The results suggested that granulocytes were responsible for most nanoparticle uptake in the blood. The nanoparticles induced the differentiation of monocytes into dendritic cells and macrophages, increasing their abundance in the blood.^[56] Although these uptake characteristics are likely different for other nanoparticle formulations, the findings of Yang et al. highlight the complexity of nanoparticle-blood interactions and warrant analysis of blood uptake patterns for novel nanoparticle formulations.

Following administration, nanoparticles are transported with the blood directly to the heart through the venous network. Nanoparticles are carried by the blood to the right ventricle and subsequently enter the pulmonary circulation. After a journey in the lung, nanoparticles return with the blood to the left atrium via the pulmonary veins and then flow into the left ventricle, from where they flow out of the heart and enter the systemic circulation, allowing interactions with various organs and tissues throughout the body.^[57]

In a healthy heart, all major immune cell types are present, with resident macrophages comprising the predominant population.^[58] These macrophages primarily reside within the myocardium, which is on the other side of the blood vessel wall, resulting in limited contact and phagocytosis of

nanoparticles.^[59] However, under pathological conditions, such as myocardial infarction or infection, there is a substantial influx of immune cells into the heart to remove dying cells and pathogens.^[58] This recruitment of immune cells can alter the nanoparticle biodistribution patterns. A significant increase of nanoparticle accumulation in the heart was observed in animal models with ischaemia-reperfusion injury.^[59,60] Specifically, the ischaemic area exhibited higher nanoparticle levels compared to the non-ischaemic area.^[60,61] Furthermore, evidence suggests that diseased hearts have enhanced vascular permeability, which may contribute to nanoparticle extravasation and accumulation.^[60,62]

3.2. Liver

The literature suggests that between 30% and 99% of administered nanoparticles are sequestered by the liver.^[4,63] This high level of nanoparticle uptake is made possible by the large portion of cardiac output received by the liver (25%), the large numbers of macrophages found in the liver (for example, $\approx 1 \times 10^7$ Kupffer cells per average adult mouse liver^[64,65]), and the liver's unique micro-architecture.^[63,66] Kupffer cells are specialized macrophages specifically resident in the liver. The liver micro-architecture is shown schematically in **Figure 3** and markedly affects the liver's nanoparticle uptake. Stellate cells and the hepatic arterial buffer response regulate liver vasodilation,^[67] resulting in 1000-fold slower blood flow in the hepatic sinusoids than in systemic circulation and an increased probability of nanoparticle-cell interactions.^[66]

Nanoparticle uptake is generally greater close to the portal triad. Kupffer cells have been shown to take up the highest number of hard nanoparticles, followed by B cells, endothelial cells, T cells, and other cell types.^[66] Unless specifically stated otherwise, within this manuscript, “hard nanoparticle” typically refers to inorganic nanoparticles, such as gold nanoparticles, quantum dots, and silica nanoparticles, whereas “soft nanoparticle” refers to organic nanoparticles, such as liposomes. Despite this trend for hard nanoparticles, other studies have shown that Kupffer cells may not contribute as much to nanoparticle clearance as initially thought, especially regarding the clearance of soft nanoparticles.^[68] The interaction between soft nanoparticles and liver macrophages needs to be further studied to determine how the uptake of liver macrophages changes based on different nanoparticle characteristics.

3.3. Spleen

Weighing an average of 150 g, the spleen is $\approx 0.2\%$ of human body weight but receives 5% of cardiac output.^[69] As shown in **Figure 4**, the spleen is divided into two main compartments: red and white pulp. The white pulp contains macrophages, lymphocytes, dendritic cells, and plasma cells, but its function is primarily related to the antigenic immune system. The red pulp contains macrophages, reticular cells, lymphocytes, hematopoietic cells, plasma cells, and plasmablasts. It is primarily tasked with removing foreign material and aged RBCs from systemic circulation. The red pulp macrophages are the most numerous resident

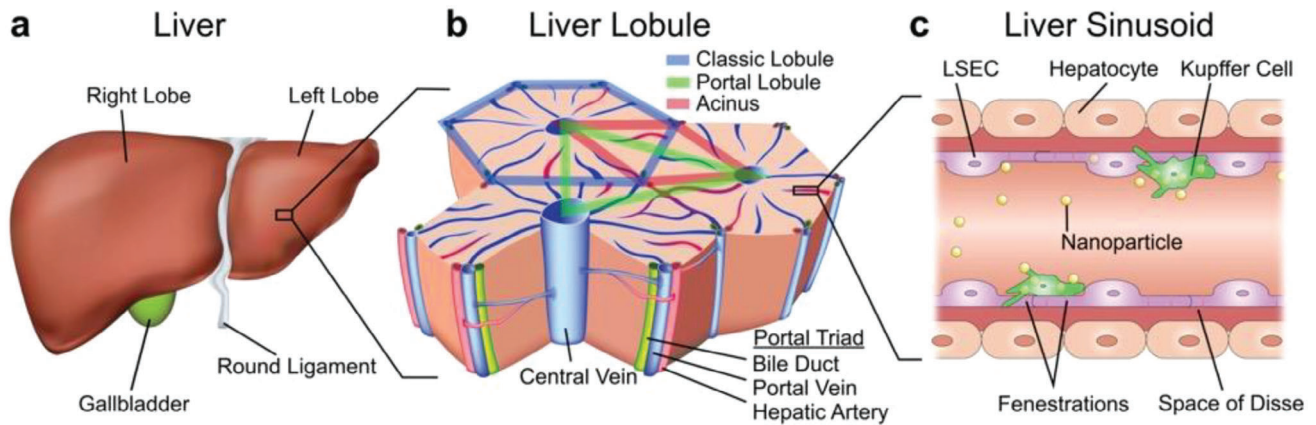


Figure 3. Schematic of the liver micro-architecture. a) The liver is composed almost homogeneously of microscopic functional units called liver lobules b). Blood flows into the liver via the hepatic veins and arteries. Together with the bile duct, these two vessels form the portal triad. Blood flows from each portal triad to the three nearest central veins, and bile flows in the opposite direction to collect in the bile duct for excretion. The classic lobule model comprises a hexagon tracing the six nearest portal triads surrounding a given central vein. The portal lobule model is visualized with a triangle connecting three adjacent central veins. The acinus model is described as a diamond shape with two portal triads on the short axis and two central veins on the long axis. The acinus model is most relevant to nanoparticle clearance as it emphasizes blood flow from the portal triads and the vessel network connecting them to the central vein. As blood flows toward the central vein, it passes through small vessels called sinusoids c). Blood velocity decreases significantly, and the blood is allowed to interact with various cell types. As shown in panel (c), nanoparticles in the blood interact with different cell types, including Kupffer cells (macrophages), fenestrated liver sinusoidal endothelial cells (LSECs), and hepatocytes. The liver sinusoids are the primary location in the body where clearance of foreign materials (including engineered nanoparticles) from the blood occurs.

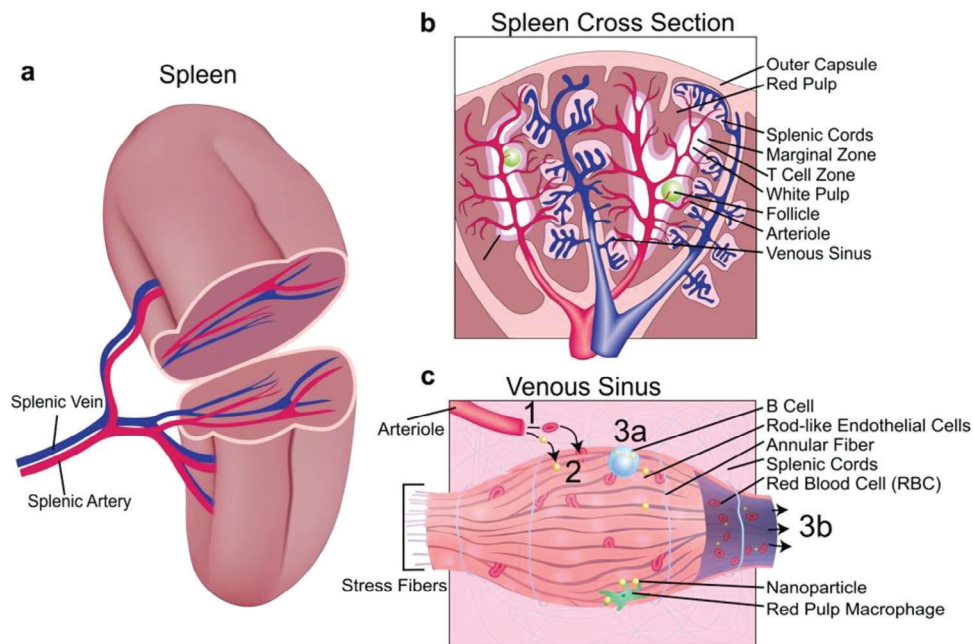


Figure 4. Schematic of the spleen micro-architecture. a) The spleen is fed by arterial blood through the splenic artery and drains through the splenic vein. Arterial blood flows through arterioles and out into the white and red pulp of the spleen. b) A small amount of blood is processed in the white pulp, where the spleen's complex lymphoid (adaptive immunity) function is carried out. Most blood flows out of the branched arterioles into the red pulp of the spleen. The blood is pushed into the splenic cords and collects in the splenic sinuses to exit the spleen. c) The splenic sinuses comprise unique, lengthened endothelial cells with parallel stress fibers and perpendicular annular fibers contributing to the spleen's filtering function. 1) Venous blood containing nanoparticles enters the splenic cords through arterioles. 2) Blood and nanoparticles flow through the splenic cords until pressure pushes them against the slits between the endothelial cells of the sinus. 3a) Nanoparticles or old RBCs that are too large or inflexible to pass through the slits will persist in the splenic cords and eventually be cleared by red pulp macrophages, B cells, and dendritic cells. 3b) Nanoparticles and healthy RBCs that are small or flexible enough to pass through the slits will exit the splenic sinus and return to circulation.

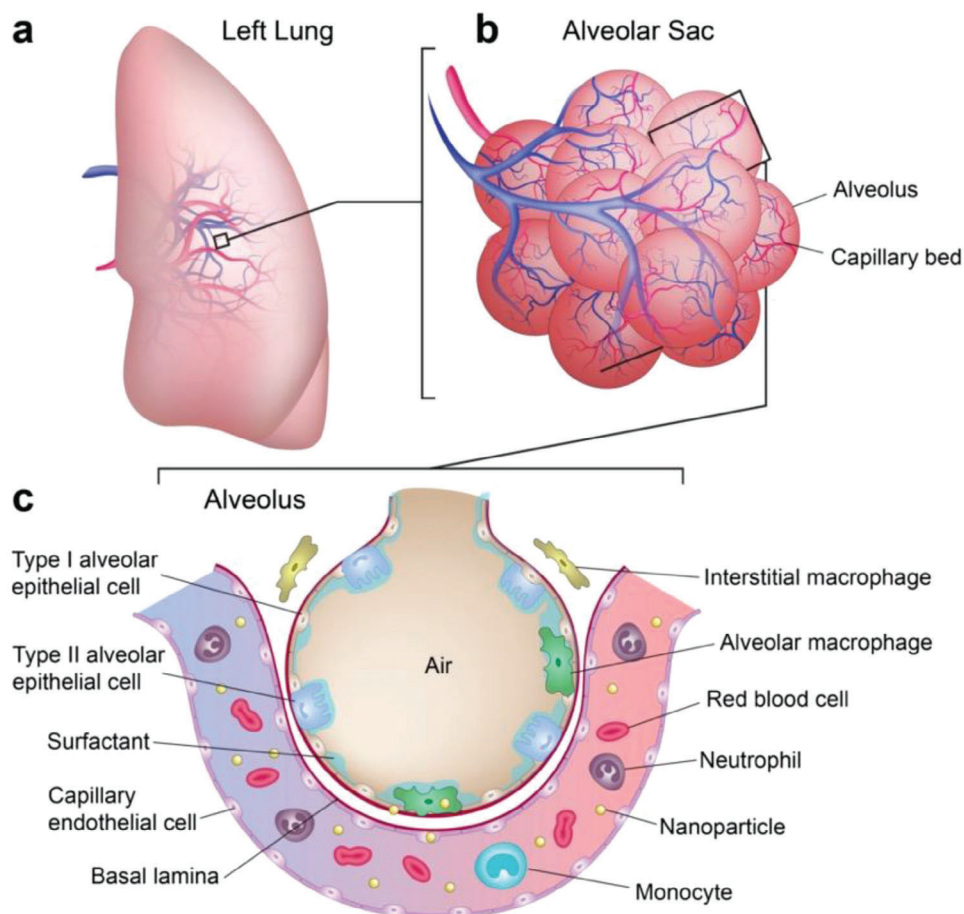


Figure 5. Schematic of the lung micro-architecture. a) The lung has the largest vasculature system in the human body, bringing about a vast endothelium surface area of almost 70 m^2 for the interaction between nanoparticles and endothelial cells. b) The lung is composed of more than 300 million alveoli. Each alveolus is covered with numerous pulmonary capillaries, forming the functional unit for gas exchange. c) Nanoparticles interact with different lung cells after systemic administration. Neutrophils, rather than intravascular macrophages, are the major immune cell type in the lung capillaries. Neutrophils do not significantly internalize nanoparticles without activation. When passing through the lung capillaries, nanoparticles interact with the endothelium. The endothelial cells are tightly aligned along the vascular wall, exhibiting no gaps or fenestrae. In general, only a small portion of systemically administered nanoparticles cross the endothelium and interact with pulmonary macrophages and alveolar epithelial cells.

macrophages of the spleen. Dendritic cells and two distinct types of macrophages in the marginal zone further have the ability to phagocytize pathogens and foreign material.^[70]

The red pulp macrophages, marginal zone macrophages, and dendritic cells actively phagocytose foreign material, including nanoparticles, passing through the arterioles and sinusoids of the spleen.^[71,72] The nanoparticle distribution within the spleen can also heavily depend on model species and nanoparticle characteristics.^[73] Nanoparticle accumulation in the spleen is assisted by the filter-like features of the splenic sinusoids (Figure 4), resulting in much higher uptake levels for nanoparticles over 200 nm in diameter.^[74] Particles hindered by the small slits in the splenic sinusoids can be subsequently taken up by various splenic cells. However, recent studies have begun to overcome the variety of splenic barriers and found that soft, zwitterionic (overall neutral surface charge due to containing an equal number of oppositely charged groups that balance each other out) nanoparticles can deform and pass between slits in the venous sinusoids of the spleen, passing back into circulation and avoiding

splenic entrapment and macrophage clearance.^[75] When large particles (e.g., 500-nm polystyrene particles) are trapped in the spleen, they are predominantly taken up by B cells. Dendritic cells are also highly involved, followed by a high number of macrophages (relative to blood and bone marrow), monocytes, and granulocytes.^[56]

3.4. Lungs

The lungs receive 100% of cardiac right ventricle output, which is venous blood from every tissue in the body.^[76] Upon intravenous administration, nanoparticles are first transported to the heart through the venous network and then enter the pulmonary capillary network (PCN) (Figure 5).^[57] The PCN is the largest vasculature system in the human body, which presents $\approx 25\text{--}30\%$ of the total endothelial surface.^[77,78] The lungs lack intravascular macrophages, which is different from the liver and spleen.

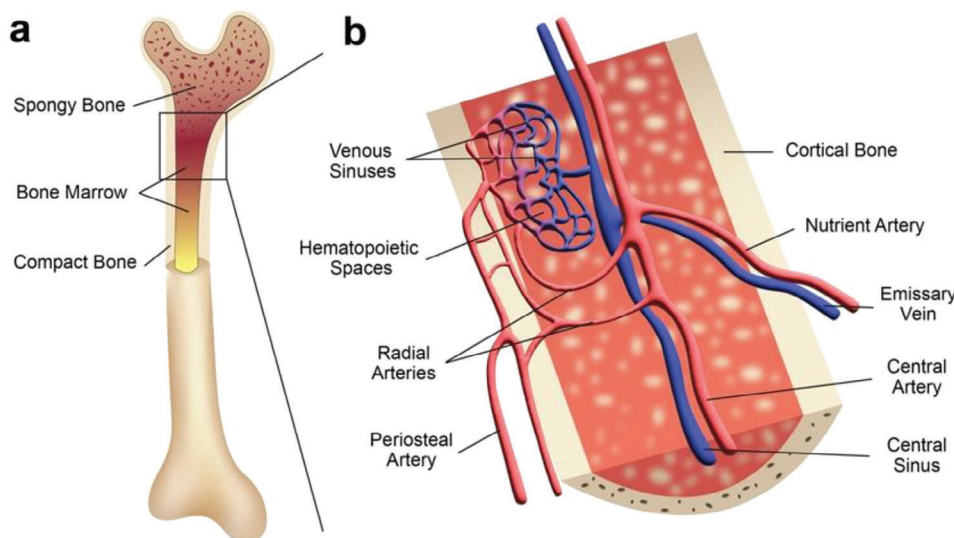


Figure 6. Schematic of the bone marrow micro-architecture. a. The bone is made up of compact bone, spongy bone, and bone marrow. Red bone marrow, where the venous sinuses locate, is mainly found in the spongy bone, while yellow bone marrow is in the central cavity of long bones. b. The primary blood supply to the bone marrow enters through the cortical bone and reaches the central artery in the medulla cavity via the nutrient artery. After meeting the periosteal arterial supply, blood drains into venous sinuses. Venous sinuses are capillary networks that support hematopoietic cells located in the hemopoietic spaces. The sinusoidal endothelium is fenestrated and is covered by an interrupted basement lamina. Mature blood cells can cross the sinusoidal endothelium and enter the bloodstream. Eventually, these sinuses converge to the central sinus, and blood exits the medullary cavity through emissary veins.

Neutrophils are the dominant immune cell type in the lungs.^[79,80] Since neutrophils are more responsive to pulmonary acute injury and inflammation, they generally do not significantly internalize nanoparticles without stimulation and activation.^[57,81] Thus, in most situations, the lungs do not accumulate large amounts of nanoparticles compared to other organs, such as the liver and spleen. After activation by inflammatory cytokines, neutrophils can internalize nanoparticles, migrate across blood vessels, and transport nanoparticles into the inflammation area.^[81]

It has been reported that lung endothelial cells interact more efficiently with nanoparticles than immune cells.^[82–84] The large surface area and small diameter of the PCN (2–13 μm) facilitate the interactions between nanoparticles and the endothelium. Additionally, the relatively slow blood flow rate through the capillaries further enhances these interactions.^[77,85]

The tissue-resident macrophages of the lungs are interstitial macrophages and alveolar macrophages (Figure 5c). Interstitial macrophages are located in the interstitium between the microvascular endothelial layer and the alveolar epithelial layer. Alveolar macrophages are localized in close contact with the alveolar epithelial layer on the air side, which are highly involved in phagocytosis and monitoring debris and pathogens from inhaled air.^[86,87] Thus, systemically administered nanoparticles do not readily interact with pulmonary macrophages, as this interaction requires nanoparticles to cross the continuous endothelial cell monolayer first. Despite this anatomical characteristic of the lungs, the uptake of systemically administered nanoparticles in pulmonary macrophages and alveolar epithelial cells has been reported.^[88] Other pulmonary immune cells, including monocytes, dendritic cells, B cells and T cells, also contribute to nanoparticle uptake in the lungs.^[82]

There are nanoparticle formulations that target the lungs.^[89,90] Polyethyleneimine (PEI)-containing polyplexes, cationic bovine serum albumin nanoparticles, and poly(β -amino esters) based nanoparticles can accumulate in the lungs through passive targeting.^[82,91–93] While GALA peptide modified nanoparticles actively target sialic acid-terminated sugar chains presented on pulmonary endothelial cells.^[88] Further, the transient aggregation of nanoparticles has been applied as a strategy for lung targeting based on size-related mechanisms.^[94] However, nanoparticle colloidal instability may induce irreversible microscale aggregation, increasing the risk of pulmonary embolism. Future research studies may explore in more detail the interactions and dynamics between systemically administered nanoparticles and the lungs.

3.5. Bone Marrow

The bone marrow is the primary hematopoietic organ and a primary lymphoid tissue, producing RBCs, various types of WBCs, and platelets. It is located in the core of bones throughout the body (Figure 6a).^[95] To supply the body with the cells it produces, it receives a significant blood flow through feeding arteries. Blood then drains through venous sinuses and exits the bone through nutrient veins (Figure 6b).^[96] The marrow sinusoidal system differs from the spleen and liver in that it comprises a thin, flat layer of endothelial cells between the bone and marrow.^[97] These endothelial cells, called marrow sinusoidal endothelial cells (MSECs), demonstrate significant endocytic behavior of particulate matter, including nanoparticles.^[98] This function is related to the splenic SECs and red pulp macrophages, as the bone marrow is similarly tasked with removing old or damaged RBCs from circulation.^[99]

The bone marrow has been reported to sequester up to 50% of systemically administered nanoparticles. Still, this uptake occurs primarily with smaller nanoparticles (<150 nm) that have evaded the liver and spleen.^[100] With larger (500 nm) polystyrene nanoparticles, Yang et al. demonstrated prolonged (>96 h) residence of nanoparticles in the bone marrow, with granulocytes dominating nanoparticle uptake. In contrast to blood-mediated nanoparticle uptake in the same study, bone marrow uptake among cell populations did not fluctuate as much with time, and double-negative (Gr-1^{neg}, Ly6C^{neg}, mostly dendritic) cells were the most efficient population in phagocytizing nanoparticles.^[56] Another study showed that CD11b+ Gr-1+ cells are recruited by polymeric nanoparticles (PLGA/OVA) in the bone marrow, and that these cells can then cross-present the nanoparticle-borne antigen, resulting in antigen-specific T cell proliferation.^[101]

3.6. Skin

The skin is the body's largest vascularized organ and carries out multiple functions, including protection, sensing, and maintaining homeostasis.^[102] Some biodistribution studies mention accumulation in the skin, usually reporting minimal accumulation compared to other organs.^[103–105] However, these studies do not mention the cells involved or the uptake mechanism in the skin. A unique study by Sykes et al. described the accumulation of gold nanoparticles and quantum dots in the skin in greater detail. This study found that nanoparticles accumulate in the skin in quantities linearly correlated with administered dose. More specifically, nanoparticles were found in dendritic cells and dermal macrophages upon administration with low doses. At the same time, they are distributed more generally in the pericellular space of the dermis and subcutaneous tissue at higher doses.^[106] The higher accumulation of nanoparticles in non-macrophage cell populations at higher doses could be due to saturation mechanisms of phagocytic cells. In addition, nanoparticles were cleared from the skin over time and drained into the lymphatic system and lymph nodes. Thus, nanoparticle accumulation in the skin and lymphatic system are closely related.^[106]

3.7. Lymph Nodes

The lymph nodes are the connecting points of the circulatory to the lymphatic system, making them integral in the functioning of both adaptive and innate immunity, antigen processing, and mounting defenses against a host of foreign pathogens. The lymph nodes contain three types of macrophages: i) subcapsular sinus macrophages; ii) medullary sinus macrophages; and iii) medullary cord macrophages.^[107] Yang et al. showed that major populations involved in polymeric nanoparticle uptake in lymph nodes include B cells, dendritic cells, monocytes, and granulocytes. However, the lymph node accumulation at 6 h was significantly lower than in other organs.^[56] Larger nanoparticles (50–100 nm) are retained for extended periods (>5 weeks) in the follicles, while smaller ones (5–15 nm) are quickly cleared in under 48 h.^[108] In addition to nanoparticle size, lymph node accumulation depends on time. At later time points (12 h), the

lymph node uptake of nanoparticles outstripped even the liver distribution.^[109] It has been suggested that lymph node accumulation may increase over time because the lymphatic system drains nanoparticle-containing dendritic cells from other tissues, such as the skin.^[106] However, nanoparticles can further get to lymph nodes through pathways other than dendritic cell-mediated transportation. For example, nanoparticles are often transported to lymph nodes as extracellular particles in the lymph.^[109]

3.8. Kidneys

The kidneys are unique among the NBRP organs because they predominantly clear nanoparticles through cell-independent mechanisms (**Figure 7**). Nanoparticles with diameters less than approximately six nanometers will be quickly cleared from circulation by the kidneys through the glomerular filtration process.^[110] However, the clearance of larger nanoparticles can be promoted by incorporating a glycan surface modification.^[111] Although some phagocytic cell types reside in the kidneys, phagocytosis and long-term accumulation are minimal compared with other organs. Further, analysis of fluorescent or radiolabeled nanoparticle uptake in the kidneys is complicated due to the kidneys' filtration of the small molecular tags used for nanoparticle detection, which may break off from nanoparticles during circulation in the body. For interested readers, nanoparticle-kidney interactions are reviewed in greater detail by Du et al.^[112]

3.9. Tumors

Due to large populations of immune cells in some solid tumors, such as tumor-infiltrating myeloid cells (TIMCs) and tumor-associated macrophages (TAMs), tumors may be viewed as another NBRP organ.^[113] This intratumoral immune cell infiltration may be a barrier to nanoparticle tumor delivery. Often, nanoparticles are taken up by TAMs rather than malignant cells.^[114] Yet, rather than presenting an insurmountable problem, nanoparticle uptake by TAMs represents an opportunity to target these tumor-associated immune cell populations for immunomodulatory cancer therapies.^[115] It has been suggested that there are at least ten subtypes of macrophages, four subtypes of monocytes, four subtypes of dendritic cells, five subtypes of neutrophils, and two subtypes of mast cells present in the tumor microenvironment.^[113] Tumor-associated macrophages are associated with good or bad cancer outcomes, presenting a host of potential targets for stimulation, suppression, repolarization, and other immunomodulatory strategies.^[113] Various reviews have described this immune-targeting strategy since at least 1988, and the idea warrants further research and development.^[116,117]

4. Nanoparticle Design Modulation

Nanoparticle design modulation includes variations of nanoparticle physicochemical properties, such as size, shape, stiffness, and

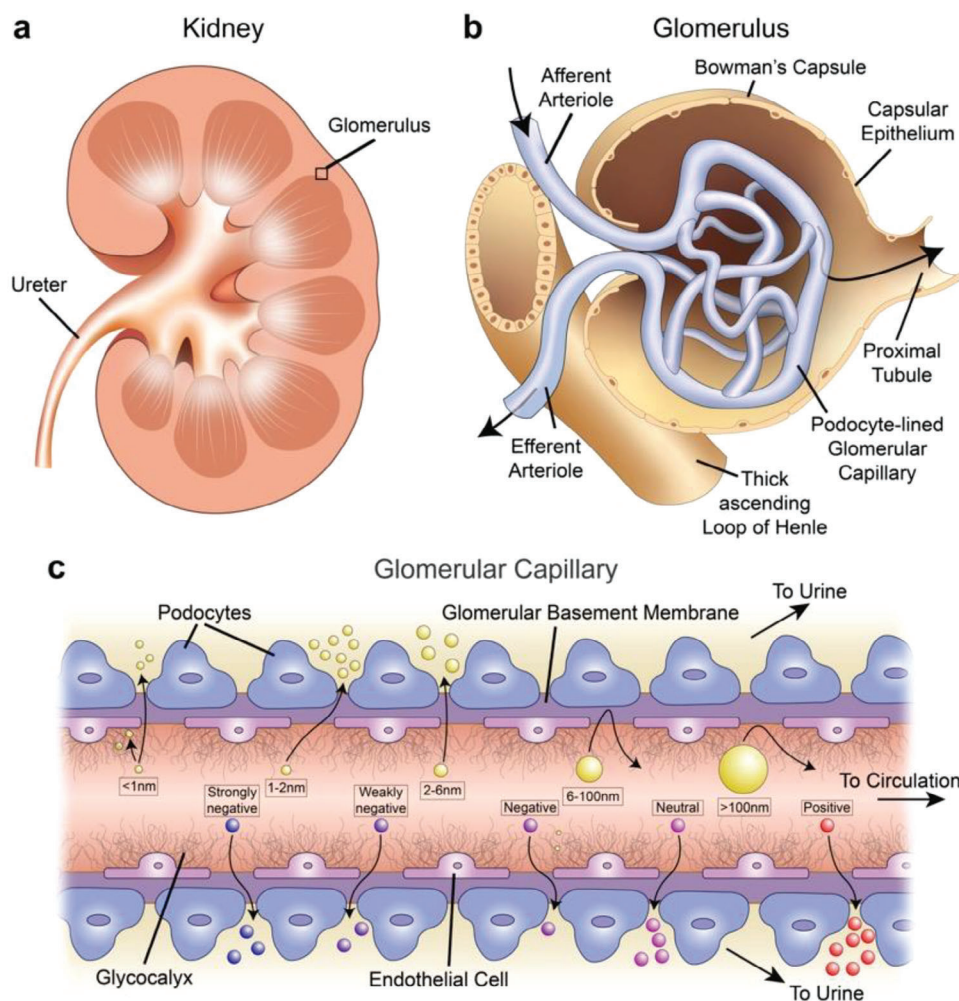


Figure 7. Schematic of kidney micro-architecture. a) The kidneys receive blood from circulation. Filtered blood exits back into circulation, and the filtrate exits through the ureter to excretion in the urine. b) The glomerulus is the functional unit of the kidney. Blood enters through the afferent arteriole, passes through the glomerular capillaries, and exits through the efferent arteriole. Particles and other waste products that exit the glomerular capillaries are collected in Bowman's capsule and then exit through the proximal tubule. c) The boundary of the glomerular capillaries comprises the vessel endothelial layer, the glomerular basement membrane, and a layer of podocytes surrounding the vessel. This boundary acts as a filtration membrane that lets nanoparticles through with different dynamics relative to their size and charge characteristics. Generally, positive particles and particles with a diameter of fewer than six nanometers experience rapid clearance and subsequent excretion in the urine.

surface properties (so-called 4S parameters).^[118] These 4S parameters significantly affect various aspects of nanoparticle-NBRP interactions in both cell-dependent and cell-independent pathways, including serum protein adsorption, phagocytic recognition and interaction, trajectory and margination (migration toward vessel walls) dynamics in vessels, endothelium adhesion and extravasation, and organ filtration, and thus play a crucial role in blood circulation duration and biodistribution of nanoparticles.^[119] While these effects have been studied extensively, it is challenging to generalize nanoparticle-NBRP interactions in part due to their mechanistic complexity and the overall lack of standardization in the literature regarding animal and disease models, procedures, and even nanoparticles themselves (Refer to Table S1, Supporting Information for several instances of controversial findings in the literature).^[120,121] Here, we review nanoparticle-NBRP interactions with an emphasis on nanoparticle size, shape, elastic-

ity/stiffness, and surface properties classified as surface charge and surface modification (Figure 8). Additionally, we summarize the impact of the nanoparticle material on nanoparticle-NBRP interactions.

4.1. Nanoparticle Size

Size is a key determinant of the biological fate, toxicity, and health effects of systemically administered nanoparticles.^[122–125] Nanoparticle size is often measured using dynamic light scattering (DLS) or imaging methods such as transmission electron microscopy (TEM).^[126]

Due to the intricate interplay of nanoparticle properties and study models, it is difficult to establish consistent and precise cell uptake trends or biodistribution patterns based solely on

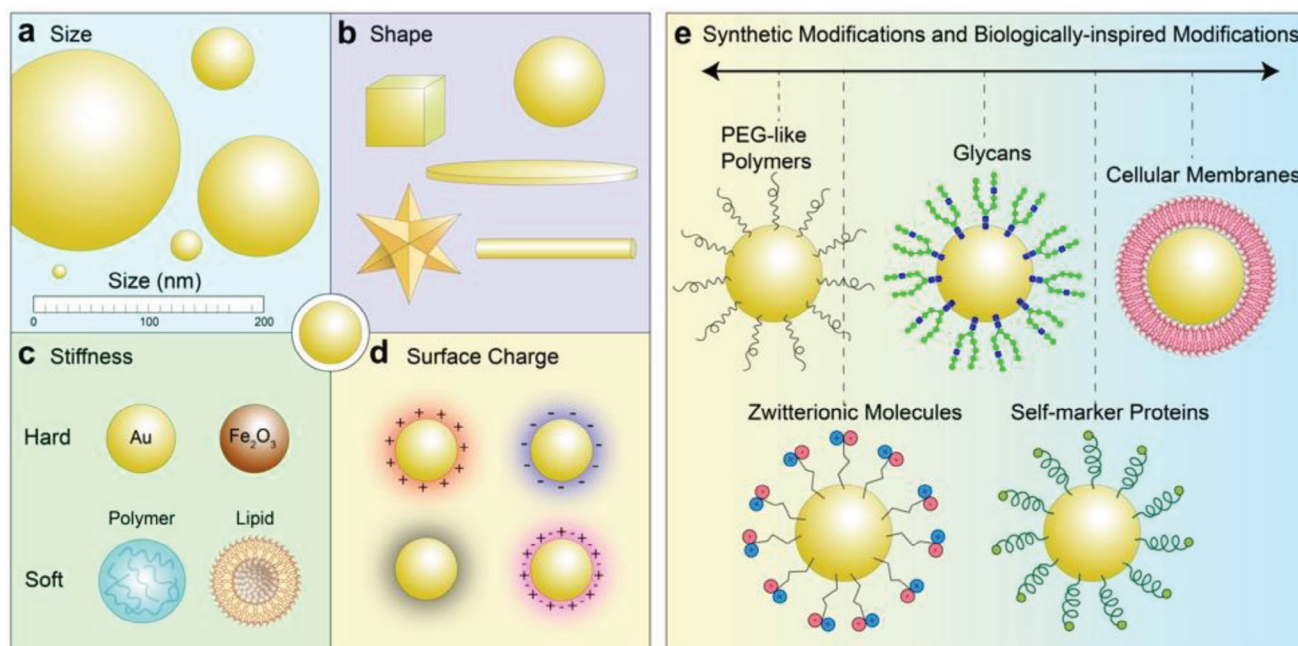


Figure 8. Nanoparticle design modulation strategies to reduce NBRP interactions and clearance. The intrinsic nanoparticle physicochemical properties, including a) size, b) shape, c) elasticity/stiffness, and d) surface charge, can be modulated to reduce uptake by NBRP organs and cells. e) Nanoparticle surface modifications exhibit a broad range of methods ranging from purely synthetic to biologically-inspired surface modifications.

size.^[127] This complexity is particularly evident when examining the impact of size on the interaction between nanoparticles and cell-dependent NBRP, such as macrophage uptake efficiency.^[128] In a certain study, larger gold nanoparticles (50 nm) exhibited higher uptake efficiency than their smaller counterparts (5 and 20 nm).^[129] Similarly, in another work, uptake efficiency increased with the augmentation of gold nanoparticle size (15, 30, 60, and 90 nm).^[130] However, in contrast, another study observed that 150 nm silica nanoparticles displayed a greater internalization rate than larger ones (250, 500, and 850 nm).^[131] This discrepancy is indeed reasonable and not difficult to anticipate. Even for nanoparticles of identical composition, shape, and surface modification, different sizes endow distinct curvatures, leading to variations in surface ligand patterns.^[130] Both nanoparticle curvature and ligand patterns influence the profile of the surface protein corona, subsequently impacting the endocytosis pathways the nanoparticles undergo to enter cells, such as macrophages.^[132] Moreover, the nanoparticle size itself can also affect the internalization pathway. The combined contribution of these factors affects the complexity of understanding and predicting nano-bio interactions.

However, some general trends can be summarized, primarily attributed to the micro-structure of cell-independent NBRP, which can serve as valuable insights for informing nanoparticle design. Small nanoparticles (<6 nm) are quickly cleared from the body by the kidneys through glomerular filtration (Figure 7c).^[133] Generally, nanoparticles of all sizes greater than 6 nm tend to accumulate substantially in the liver and spleen. In the 6–100 nm size range, smaller nanoparticles tend to distribute more equally into multiple organs, while larger ones tend to have a higher accumulation in the liver and spleen.^[134,135] Based on the geometry of the splenic sinusoid endothelial cells (Figure 3c), nanoparti-

cles with >200 nm diameter would be expected to be trapped by the spleen. Indeed, splenic distribution has been shown to increase with sizes up to ≈ 200 nm,^[136] but some studies report a decrease in splenic accumulation for larger sizes.^[137] This discrepancy could be caused by increased nanoparticle uptake by the lungs, liver, and other NBRP organs before reaching the spleen.^[4] Additionally, larger nanoparticle sizes can exhibit limited penetration into tumor tissues.^[138]

4.2. Nanoparticle Shape

In addition to size, the geometric structure can significantly influence nanoparticle interaction with NBRP, affecting cellular uptake, dynamics in blood flow, and organ distribution.

Despite the prevalent focus on spherical particles in many studies and clinical applications, a diverse body of literature suggests that non-spherical shapes exhibit longer circulation times and lower degrees of internalization by NBRP cells.^[139] Generally, spherical nanoparticles are more susceptible to phagocytosis by macrophages than discoidal and rod-shaped nanoparticles, although the latter two particles typically have higher attachment with cell plasma membrane than the former ones.^[128,140] This trend is generally consistent for larger particles at the micrometer scale.^[141] However, for nanoparticles, this rule is less applicable, and contradictory findings are reported in the literature. For instance, elongated PLGA particles at both 150 nm and 2 μ m showed significantly reduced uptake by J774.A1 macrophages in one study.^[142] In contrast, another study observed that primary macrophages and monocytes engulfed nearly equal amounts of PEGylated spherical gold nanoparticles (15 or 50 nm) and gold nanorods (15 \times 50 nm).^[141,143] Furthermore, in yet

another study, Raw 264.7 macrophages associated more with silica nanocylinders ($\approx 200 \times 400$ nm) than nanospheres (≈ 200 nm) after a 2 h incubation.^[144] In vivo studies generally present that non-spherical nanoparticles have longer circulation times. For a comprehensive understanding of the effect and mechanism of nanoparticle shape on NBRP cell interactions and the associated controversies, we refer readers to comprehensive review papers.^[128,141]

From a hemorheological perspective, nanorods, nanoworms, and nanodisks display hydrodynamic behavior markedly different from spherical nanoparticles in blood flow. Specifically, filamentous, string-like nanoparticles, such as nanoworms and filomicelles, may orient themselves in the direction of blood flow and distribute mainly in the center of flow, decreasing interactions with NBRP cells on the vascular walls or in sinusoids.^[145] This contributes to an extended blood circulation time of nanoparticles with such filamentous geometry. Notably, Discher and colleagues have demonstrated that filamentous polymer micelles exhibit extended circulation lasting over a week after administration.^[146] In contrast, the spherical counterparts typically have much shorter circulation times of ≈ 2 to 3 days. Discoidal particles, on the other hand, follow unique tumbling and rolling migration routes in blood flow, increasing their association with vessel walls.^[10] This enhanced margination dynamics of discoidal particles facilitates particle-endothelial cell binding, ligand-receptor recognition, and extravasation through the discontinuous endothelial layer in tumor vasculature.

The interaction between nanoparticles with various shapes and NBRP-organs can be inferred from their biodistribution profiles.^[141] Short rods and spherical nanoparticles generally accumulate in the liver. Nanoparticles with higher aspect ratios tend to be filtered out by the spleen.^[147] In the spleen, the distribution preference follows the order of long rods > short rods > spheres.^[141] Discoidal particles have been shown to accumulate in the lungs, possibly due to their improved margination behavior and the narrow vessels in the extensive pulmonary capillary network.

4.3. Nanoparticle Elasticity/Stiffness

Nanomaterial mechanical properties are important characteristics that can influence biological interactions.^[148] Among these properties, the most studied for nanoparticles are elasticity and stiffness. Nanoparticle elasticity is an intrinsic property of the material and is commonly quantified by the Young's Modulus, which measures a material's deformation in response to applied pressure.^[149] Nanoparticle stiffness, besides material elastic modulus, is also affected by the physical and chemical structures and geometries.^[150] Although elasticity and stiffness exhibit different definitions and equations in physics, high elasticity (or stiffness) is generally associated with harder (or stiffer) materials, while low elasticity (or stiffness) is with softer and more flexible ones. The main types of tunable elastic nanoparticles include hydrogel nanoparticles and hybrid polymer-lipid nanoparticles.^[150] Nanoparticle elasticity/stiffness can influence blood circulation and biodistribution by modulating interactions with NBRP cells and NBRP organ filtration processes.^[151]

Numerous studies have described interactions of nanoparticles of varying elasticity with multiple cell lines, but no simple and consistent conclusion could be drawn from the results. The majority of studies reported that macrophages uptake stiff nanoparticles more efficiently than less elastic ones, which is one of the reasons why less elastic nanoparticles generally have longer blood circulation.^[150] The possible mechanism is that less elastic nanoparticles are easier to deform, which decreases the membrane wrapping efficiency during endocytosis.

The effect of elasticity on internalization by other cells in the body and tumor cells is controversial in the literature. For example, lower elasticity can lead to decreased cellular internalization for (polymer core-lipid shell) nanoparticles in both tumor and endothelial cells, which is consistent with the trend seen in macrophages.^[152] However, less stiff hollow silica nanocapsules showed greater uptake in tumor cells compared to stiff silica nanoparticles.^[153] Shen et al. reported that membrane wrapping efficiency might be a function of both receptor diffusion kinetics and thermodynamic driving forces, meaning that besides elasticity/stiffness, the cell internalization kinetics for nanoparticles also depends on size and shape.^[154]

Furthermore, endocytosis is not the only strategy by which nanoparticles enter cells. There is a report that less elastic liposomal nanoparticles can be internalized by tumor cells through fusing with cell membranes, which requires less time and energy than the stiff counterparts that internalize through endocytosis.^[155] The complexity of interacting factors (e.g., material, nanoparticle size and shape, and cell type) may account to some extent for the variation in results seen in different studies.

Nanoparticle elasticity/stiffness does affect not only interactions with NBRP cells but also interactions with NBRP organs. Especially salient are nanoparticle interactions with the spleen. As a result of the filter-like anatomical microstructure previously described, less elastic nanoparticles can deform and squeeze through the slits between the endothelial cells of the splenic sinus, much like healthy RBCs.^[156] This phenomenon also contributes in part to the prolonged blood circulation of soft nanoparticles.^[150]

The elasticity/stiffness also plays a crucial role in nanoparticle margination in blood flow. In general, rigid nanoparticles tend to exhibit enhanced margination compared to the corresponding less stiff ones.^[157,158] This phenomenon is particularly evident at high shear rates. On the other hand, in low shear rate regimes, deformable nanoparticles exhibit comparable, even slightly superior, margination compared to rigid counterparts.^[157,158] The margination effect is reported to be stronger for microscale particles than for nanoscale particles.^[159–161] It is important to recognize that the margination effect is multifaceted and influenced by not only particle properties, including size, shape, surface modification, and stiffness, but also vascular characteristics, such as shear rate, vessel diameter, and hematocrit level.^[110,158,159,162,163] The human circulatory system is heterogeneous, consisting of blood vessels with a wide range of flow rates and vessel diameter in different organs. Therefore, a careful and comprehensive consideration of these factors is imperative.

4.4. Nanoparticle Surface Charge

Nanoparticle surface charge, often measured as the zeta potential, is another physicochemical property that affects nanoparticle interactions with NBRP cells and organs.^[164] Surface charge primarily impacts interactions with cells through two key mechanisms, electrostatic interaction and the formation of protein corona. Positively charged nanoparticles (>10 mV) tend to exhibit higher cellular internalization compared to negatively charged (<10 mV) and neutral nanoparticles (−10 to 10 mV).^[165,166] This cationic surface modification strategy has been employed to increase the cellular uptake of nanoparticles. One key rationale behind this strategy lies in the fact that positively charged nanoparticles bind more strongly to negatively charged cell membranes.^[166] This binding, however, is typically non-specific and applicable across various cell types, including those in NBRP.

Surface charge plays a vital role in nanoparticle interactions with macrophages by impacting the formation of the protein corona, which includes opsonins.^[119] Notably, nanoparticle surface charge influences both the types and quantities of adsorbed plasma proteins. Walkey and co-workers established a library of 105 surfaced-modified gold nanoparticles.^[167] They found that nanoparticles modified with positive or negative ligands absorbed more proteins than those modified with neutral ligands, thereby increasing their susceptibility to opsonization and subsequent clearance. Additionally, highly charged nanoparticles, especially positively charged ones, tend to aggregate when exposed to serum proteins post-administration.^[166] This increased size favors recognition and phagocytosis by macrophages, resulting in faster clearance compared to neutral ones.

Further, nanoparticle surface charge affects the uptake mechanisms of various cell types.^[46,168,169] With some exceptions, positive nanoparticles often employ diverse mechanisms, while negatively charged nanoparticles are more likely to use caveolae-mediated endocytosis.^[170] However, it is challenging to generalize how nanoparticle surface charge affects these underlying cell uptake mechanisms, and even contradictory results between studies have been reported (see Table S1, Supporting Information).^[120]

Taking these factors into account, nanoparticles with an overall neutral surface charge tend to have longer plasma half-lives and slower accumulation kinetics in NBRP organs compared to nanoparticles with negative or positive surface charges.^[12,110] For instance, research by Levchenko et al. showed that liposomes with a more neutral surface charge exhibited slower clearance from the blood than negatively charged liposomes (≈ -40 mV) that accumulated more in the liver.^[171] Surface charge can also influence the sub-organ distribution of nanoparticles in the liver, with different hepatic cell types displaying varying uptake preferences.^[4] Kupffer cells and LSECs are rich in scavenger receptors on their surfaces, exhibiting strong binding with negatively charged nanoparticles. In contrast, hepatocytes have been reported to distinctly prefer the internalization of positively charged nanoparticles. A study involving gold nanoparticles revealed distinct localization patterns in the spleen, with positively or negatively charged nanoparticles tending to accumulate in the red pulp, while nanoparticles with neutral charge tend to accumulate in the white pulp.^[172] In the context of glomerular fil-

tration, nanoparticles are cleared in a charge-dependent manner, with positively charged ones being cleared most rapidly, followed by neutral ones, and then negatively charged ones.^[112] This differential clearance rate arises from varying electrostatic interactions with the negatively charged endothelial glycocalyx, basement membrane, and podocyte (Figure 7c) during the filtration process.

4.5. Nanoparticle Surface Modification

The nanoparticle surface design plays a major role in directing interactions with the NBRP.^[173] The nanoparticle surface can be modified with simple polymers to biologically-inspired ligands and complex membrane structures. These compounds determine the nanoparticle fate by influencing the protein corona composition and nanoparticle interactions with specific biological entities.^[46,119] A substantial part of endeavors in surface modification aimed at attenuating recognition and clearance by NBRP cells, thereby improving the pharmacokinetics of nanomedicine. Various surface modifications for this purpose can be broadly grouped into two categories by their mechanism of action. The first category is oriented toward preventing opsonization with notable modifications, including poly(ethylene glycol) (PEG) and zwitterionic ligand. The second category aims to disguise nanoparticles as “self” entities. Typical modifications are albumin, “self-marker” protein/peptide, and cell membrane.

One of the most common surface modification methods for minimizing nanoparticle interactions with biomolecules and biological systems is PEGylation.^[174] PEGylation involves conjugating PEG to the nanoparticle surface via chemical methods.^[175] PEGylation reduces nanoparticle interactions with the biological environment through steric inhibition and the formation of an aqueous layer around the nanoparticle due to its hydrophilic nature.^[176] PEG backfilling can be used to prevent PEG from covering nanoparticle targeting moieties attached to the surface.^[177]

Additionally, it has been suggested that the optimum PEG molecular weight to minimize macrophage recognition is 2 kDa.^[178] PEGylation has been widely researched and is known to increase nanoparticle plasma half-lives of numerous formulations, but new research points to potential clinical challenges that may limit its effectiveness.^[179,180] Pre-existing anti-PEG antibodies have been reported in some humans, potentially leading to allergic reactions and accelerated blood clearance of PEGylated nanomedicines.^[181–183] A large body of literature reports alternative polymers for nanoparticle surface modification, such as polysarcosine, poloxamers, poloxamines, and polysaccharides.^[184–187] Proteins and other biomolecules can be conjugated to polymer-modified nanoparticle surfaces using efficient chemical reactions.

Another interesting nanoparticle surface modification strategy relies on the conjugation of zwitterionic ligands. These moieties consist of positively and negatively charged chemical groups, resulting in the overall presentation of a neutral surface charge.^[188] A variety of studies have reported encouraging colloidal stability of zwitterionic nanoparticle surfaces under physiological conditions with excellent stealth properties.^[189–193] However, not all zwitterionic formulations successfully evade the NBRP. For example, one study found that a zwitterionic gold

nanoparticle formulation accumulated extensively in the liver and in the spleen.^[194]

An additional surface modification technique that uses the plasma protein serum albumin can improve nanoparticle pharmacokinetics. Serum albumin is involved in the formation of the hard corona and competitively inhibits adherence of more biologically active serum components such as some opsonins and antibodies.^[195] Other techniques are even more biologically specific. One such example is the coating of nanoparticles with “self-marker” proteins like CD47 or its derived peptides, which are generally recognized by macrophages and lymphocytes, to avoid phagocytosis of healthy cells.^[30,196] When these specific biological molecules are used, nanoparticles can be rendered “invisible” to the cell types that recognize those markers.^[197]

An approach that aims at less biological specificity is the encapsulation of nanoparticles in cell membranes that already exhibit a plethora of diverse self-molecules on their surface.^[198] This approach has a great degree of biological inspiration, directly using a cell membrane as a trojan horse for nanoparticles to evade a wide variety of specific and nonspecific NBRP interactions.^[199] It has been reported that the prolonged circulation induced by RBC membrane coating outperformed the active targeting strategy, and exhibited better nanoparticle accumulation and therapeutic efficacy in hepatocellular carcinoma.^[200] In another study, researchers modified liposome surfaces with natural regulators of complement activation (RCAs), Factor I, with which the mammalian cells and some microbes avoid complement attacking. This liposome surface modification efficiently prevented complement protein C3 opsonization and the consequent cascade activation and clearance by the RES.^[201]

For a thorough understanding of the different categories of nanoparticle surface modifications and their effects on nanoparticle *in vivo* behavior, we refer the reader to recent reviews on the subject.^[119,165,166]

4.6. Nanoparticle Material

A wide range of materials is used to make nanoparticles and nanomedicines, including metals, such as gold and silver, metal oxides, such as iron oxide, organic polymers, such as poly(lactic acid) (PLA) and poly(lactic-co-glycolic acid) (PLGA), and biomolecules such as lipids, proteins, carbohydrates, and nucleic acids.^[202–206] Because nanoparticles are usually decorated with surface molecules, the specific interactions of the various material types with serum proteins and NBRP cells are difficult to characterize *in vivo*. Despite this difficulty, the effect of nanoparticle composition on cell interactions has been reported in some studies. For example, an increased cholesterol content in liposomes has been linked to the generation of reactive oxygen species (ROS) and apoptosis in macrophages.^[207]

Recently, Siegwart et al. reported selective organ targeting (SORT) nanoparticles for tissue-specific mRNA delivery and CRISPR-Cas gene editing.^[90] By adding specific SORT lipid molecules to lipid nanoparticles, the authors demonstrated selective targeted nanoparticle delivery to the lung, spleen, and liver to selectively edit therapeutically relevant cell types in these organs. The authors hypothesized that the organ-specific targeting was accomplished through tuning the internal charge

of the synthesized lipid nanoparticles rather than relying on the external charge modifications. In a follow-up study, the researchers reported that the targeting mechanism was governed by the chemical properties of the SORT molecules, which determined the specific proteins recruited onto the nanoparticle surface. The protein corona characteristics subsequently determined the nanoparticle destination through receptor recognition in the targeted organs.^[208]

The nanoparticle core material can also influence the composition and characteristics of the protein corona. Gref et al. demonstrated this by fabricating polymeric nanoparticles with different core materials but identical surface PEG molecules. These nanoparticles exhibited similar protein adsorption patterns, but the quantities of each protein varied.^[209] Walkey et al. calculated the similarity of the protein corona composition around gold and silver nanoparticles and discovered that the core material had a greater influence than core size or surface chemistry. They explained that even though the core material does not directly interact with the surrounding biological environment, it plays a crucial role in determining the density, arrangement and orientation of the attached surface molecules.^[167]

5. Biological Modulation

To control nanoparticle interactions with the NBRP organs and cells, biological modulation strategies that involve priming the body instead of engineering nanoparticle physicochemical properties have been reported. Biological modulation primarily focuses on NBRP cells, and the strategies can be divided into three broad categories as shown in **Figure 9** and Table S2 (Supporting Information): i) the cell uptake saturation strategies; ii) the use of drugs to inhibit nanoparticle endocytosis in NBRP cells; and iii) the so-called “suicide strategies” that use drugs to kill tissue macrophage populations directly. Afterward, the strategies related to cell-independent NBRP modulation are briefly summarized.

5.1. Cell Uptake Saturation Strategies

Although the NBRP can process multiple doses of administered nanoparticles over a long period,^[210] it has a short-term capacity that is naturally limited by the amount and rate of foreign material each cell can internalize. One study by Liu et al. showed that overloading the NBRP with blank liposomes could increase tumor accumulation of iron nanoparticles two-fold.^[211] This strategy could represent a way to increase nanoparticle circulation time with a relatively low-toxicity pretreatment and warrants further development and study.^[212]

Ouyang et al. reported a nanoparticle dose threshold that nonlinearly decreased liver clearance, prolonged nanoparticle plasma half-life, and increased nanoparticle tumor accumulation.^[65] Based on preclinical mouse studies, the researchers discovered that 1 trillion nanoparticles are a suitable bolus dose to overwhelm Kupffer cell uptake rates, resulting in up to 12% nanoparticle tumor delivery efficiency and nanoparticle delivery of up to 93% of tumor cells. Mechanistically, the nanoparticle dose threshold was correlated with the number of available receptors

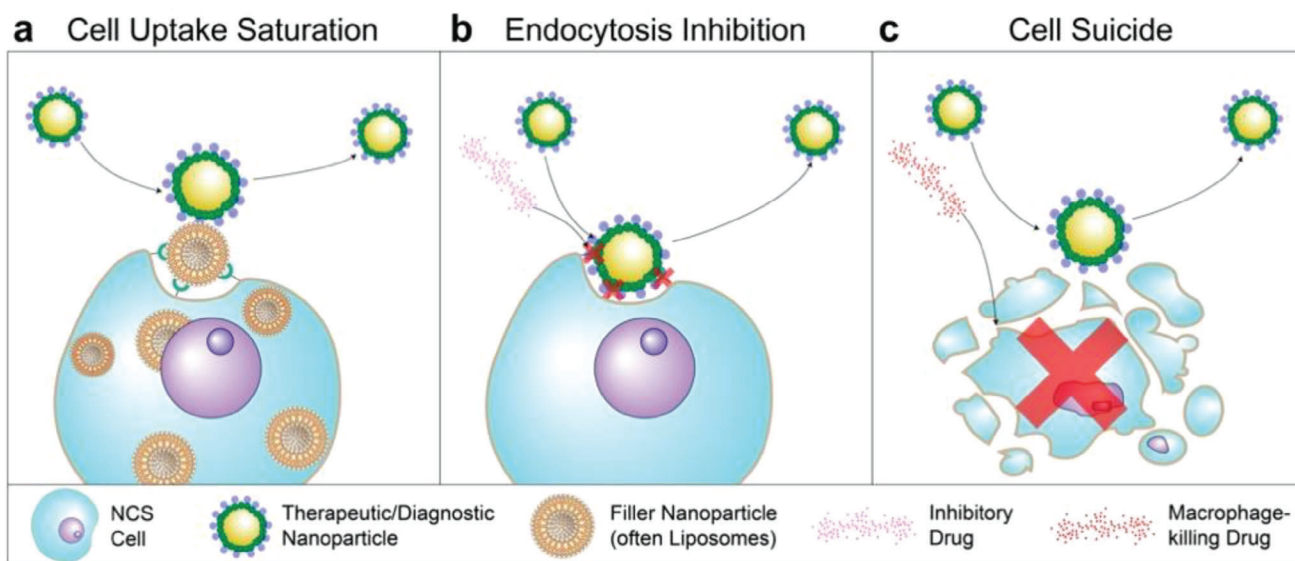


Figure 9. Biological modulation strategies. a) Saturation preconditioning strategies work by overloading NBRP cells with a non-therapeutic nanoparticle, i.e., filler nanoparticle. The nanoparticle used for saturation is usually chosen to be nontoxic and should degrade quickly after a period of time. Since NBRP cells are full of the saturating nanoparticle and/or their uptake rates are saturated, these cells cannot further engulf more nanoparticles, allowing subsequently and/or simultaneously administered therapeutic/diagnostic nanoparticles to evade the NBRP and distribute more effectively to target tissues. b) Endocytosis inhibition strategies use drugs that block the interactions between NBRP cells and nanoparticles. One mechanism is the disruption of endocytosis mechanisms by blocking receptor-nanoparticle corona interactions. Nanoparticles escape attachment to NBRP cell membranes and are free to interact more efficiently with target tissues. c) In the cell suicide strategy, drugs induce cell death in all or part of resident tissue macrophage populations, resulting in reduced nanoparticle sequestration by the NBRP.

and binding sites on Kupffer cells. While the specific cell membrane receptors involved were not reported, the data suggested that nanoparticle doses beyond the available binding site threshold overwhelmed the uptake rates of Kupffer cells, reduced liver clearance, and prolonged nanoparticle circulation.

Other than nanoparticles, a series of inorganic and organic materials, including dextran sulfate (500 kDa),^[213,214] natural polysaccharides, such as fucoidan^[215] and carrageenan,^[216] colloidal carbon,^[214] and fat emulsion,^[217] have also been applied as pretreatment reagents for NBRP function blockade. These techniques successfully improved the circulation time and performance of the nanoparticles injected afterward.

An additional cell uptake saturation method was reported by Nikitin et al. They showed that a forced clearance of the body's own intact erythrocytes using a low dose of allogeneic anti-erythrocyte antibodies increased the circulation half-lives of a range of short-circulating and long-circulating nanoparticle formulations by up to 32-fold.^[218] This MPS-cytoblockade strategy may enable novel nanoparticle-based theranostic approaches and have even further applications in fundamental life-science research.

Strategies aimed at achieving cellular uptake saturation are generally considered safe and non-disruptive to the innate immune system. These approaches function by transiently blocking the receptors responsible for phagocytosis, without compromising the overall functionality of macrophages or subjecting them to invasive depletion, as seen in alternative strategies introduced subsequently.^[4] However, it is essential to acknowledge that this approach comes with its set of limitations. To attain a sufficient saturation effect, a high dose of blocking nanoparti-

cles or materials is inevitable, which raises concerns related to dose-dependent toxicity.^[219] Additionally, macrophage functionality restores rapidly through digesting the phagocytic entities and typically fully recovers within 48 h, restricting the effectiveness and administration window for the subsequent nanoparticle treatments.^[4]

5.2. Endocytosis Inhibition Strategies

Various drugs have been shown to inhibit the phagocytic mechanisms of the NBRP. These drugs include chloroquine, gadolinium(III) chloride, and methyl palmitate.^[45,220–222] Chloroquine and gadolinium(III) chloride work by inhibiting the nanoparticle endocytosis mechanisms of macrophages.^[221] Wolfram et al. chose chloroquine as a drug candidate from other known phagocytic inhibitors and demonstrated a decrease of accumulation in the liver by $\approx 29\%$ for liposomes (from $\approx 65\%$ to $\approx 46\%$ of the total detected fluorescence signal) and 22% for discoidal silicon particles (from $\approx 73\%$ to $\approx 57\%$ of injection dose).^[223] Similarly, Deorukhkar et al. used gadolinium(III) chloride to mitigate the accumulation of quantum dots in the NBRP and increase their efficiency as an imaging agent for tumors.^[224]

The inhibitory strategies employed here are less aggressive when compared to cell suicide strategies. Nevertheless, these endocytosis inhibitors lack specificity in targeting NBRP cells, potentially leading to unintended adverse effects on other cells and organs.^[45,225] Furthermore, these inhibitors consist of ions or small molecules, which do not elicit as robust a recognition response from macrophages when compared to larger foreign

substance like liposomes and 500 kDa dextran sulfates. Consequently, their suppressive efficacy is further compromised. In a novel approach, methyl palmitate nanoparticles were fabricated by combining them with a structural compound, serum albumin.^[219] The internalization of all tested nanoparticles of different sizes, shapes, and compositions was efficiently inhibited after pre-treatment with methyl palmitate nanoparticles.

5.3. Cell Suicide Strategies

Several other drugs have been used to deplete tissue macrophage populations. One drug commonly used for this purpose is clodronate. The technique of using clodronate encapsulated liposomes to deplete liver macrophages was first developed by van Rooijen et al.,^[226,227] which was then exploited as an efficient tool to unravel macrophage functions in immunology. Later, Hao et al. used clodronate liposomes to deplete liver macrophages and improve the biodistribution of Paclitaxel-PLGA nanoparticles. Macrophage populations subsequently recovered, and minimal toxic side effects were observed during the study.^[228] Chan et al. showed that pretreatment with clodronate liposomes effectively decreased the uptake of nanoparticles by Kupffer cells in the liver.^[229] This technique has been used in other studies to reduce nanoparticle accumulation in the liver, increase circulation time, and increase tumor accumulation of intravenously administered nanoparticles.^[230,231]

Cell suicide strategies are the most effective means of incapacitating NBRP cells, but they also represent the most aggressive approaches. It has been reported that the repopulation time of liver Kupffer cells to their normal levels ranges from a few days to more than ten days, depending on the dosage administered.^[229] Macrophages play a pivotal role in the innate immune system. During this re-population period, the integrity of the host's immunity become compromised, increasing the susceptibility to pathogen infection.^[229] Therefore, when using clodronate liposomes, the researchers should carefully determine the administration route, timing, and dose. By choosing different injection routes, liposomes accumulate and deplete macrophages in particular organs.^[227,232] Intravenous and intraperitoneal administrations generally result in macrophage depletion in the liver and spleen. In addition, it has been reported that repeated and high dosing of clodronate liposomes induced severe adverse effects and even death in mice, indicating that pilot toxicity assays in experimental animals may be necessary.^[233] Besides clodronate, propamidine-containing liposomes have also shown the capability for depleting Kupffer cells, which was ten times as effective as clodronate-containing ones.^[234]

5.4. Cell-independent NBRP Modulation Strategies

A significant portion of cell-independent NBRP modulation research is centered on tuning the function and structure of tumor vasculature to enhance the delivery of nanoparticles to tumor. Priming the tumor with mild hyperthermia can increase the permeability of tumor blood vessels.^[235] Similar concepts include locally depleting tumor-associated platelets, which repair the leaky blood vessels, or depleting pericytes, which support the vessel

wall integrity by aligning with endothelial cells.^[236–238] Another avenue of investigation focused on employing anti-angiogenic agents to normalize tumor vasculature. This normalization process can reestablish the pressure gradient between vessel lumen and tumor interstitium, a critical factor for facilitating nanoparticle extravasation into solid tumors.^[239]

Studies involving the priming of healthy NBRP organs are relatively scarce, possibly due to concerns about potential disruption to the normal physiological structure and function of essential organs, such as the liver and spleen. Nonetheless, it has been reported that the blood velocity in liver sinusoids is ≈ 1000 times slower than in the general circulating bloodstream.^[66] This reduced velocity significantly increased the interaction opportunities between nanoparticles and liver resident macrophages, thus promoting nanoparticle sequestration from circulation. A similar correlation has been observed in the spleen. The blood velocity in the red pulp, enriched with macrophages and a primary site of nanoparticle accumulation, is much slower than in other regions of the spleen.^[66] Based on the above reports, increasing the blood flow rates in the liver and spleen presents a potential strategy for reducing nanoparticle clearance by the NBRP and may potentially minimize the undesirable distribution of administered nanoparticles in non-diseased organs.^[66]

Additionally, complement inhibitors have shown promise in mitigating nanoparticle clearance by NBRP cells.^[240,241] Inhibiting C3 opsonization through complement convertase inhibitors, like compstatin, soluble CD35, and soluble CD55 have effectively blocked the sequestration of iron oxide nanoparticles by leukocytes.^[242] In another work, soluble CD55 successfully suppressed the C3 opsonization in clinically approved nanomedicines, including Feraheme, LipoDox, and Onivyde.^[243] It is worth noting that these experiments were conducted in vitro using human blood, and further in vivo investigations are essential to more comprehensively assess the safety.

6. Literature Survey

Understanding the numerous factors influencing nanoparticle interactions with the NBRP is critical to assessing nanomedicine's current limitations and opportunities. Upon systemic administration, it is well established that nanoparticles distribute throughout the body with unique pharmacokinetics and biodistribution patterns. However, how does nanoparticle design affect these parameters? Generally, long nanoparticle blood circulation time and the reduction of liver accumulation are the primary goals of NBRP evasion strategies. The rationale is that if nanoparticles circulate in the bloodstream for a longer time, the chance of nanoparticle accumulation in targeted organs and tissues increases, which is beneficial for diagnostic and therapeutic applications.

To address the above question, we surveyed the recent literature. We focused on nanoparticle applications in mouse models, which are often used for preclinical nanomedicine studies (Figure 9). Our work aims to understand nanoparticle-NBRP interactions to identify nanomedicine design guidelines that improve in vivo delivery.

The literature survey methods are described in Section S1 (Supporting Information). By searching SciFinder and Google Scholar databases with the keywords “nanoparticles”,

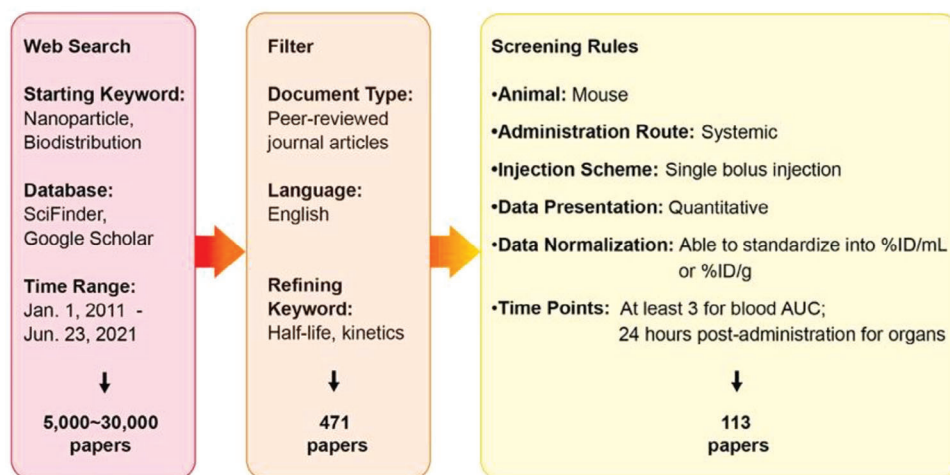


Figure 10. Procedures and filters used for the literature analysis. Peer-reviewed publications from 2011–2021 were screened and systematically organized based on their reported nanoparticle pharmacokinetics and organ distribution data. A total of 113 adequate papers were identified.

“biodistribution”, “half-life”, and “kinetics”, we identified 471 published studies since 2011. We used 113 studies for the subsequent analysis following the screening procedure outlined in **Figure 10**. We then extracted data about the reported nanoparticle physicochemical properties, pharmacokinetics, and the biodistribution for >200 nanoparticle systems (Data S1, Supporting Information). The extracted data were standardized between the different studies. Next, we organized the compiled data into categories, as shown in **Table 1**.

6.1. Nanoparticle Pharmacokinetics

We observed inconsistencies in the reported pharmacokinetics assessments among the compiled studies. Specifically, different metrics were used to present nanoparticle pharmacokinetics in different studies, such as half-life, mean residence time, maximum concentration (C, area under the curve from zero point to last time point (AUC_{0-t}), or area under the curve from zero point to infinity ($AUC_{0-\infty}$). Often, these metrics were obtained

based on different pharmacokinetic models (non-, one- or two-compartmental models, physiologically based pharmacokinetic (PBPK) model).

Therefore, to enable the inter-study comparison, we standardized the reported pharmacokinetic parameters across all compiled studies by recalculating the $AUC_{0-\infty}$ (with the unit $\%ID \cdot h/mL$, where $\%ID$ is the percentage of the injected dose, h represents hours, and mL is milliliter) of the extracted nanoparticle blood concentration ($\%ID/mL$) versus time (hours) curves based on a non-compartmental analysis model (**Figure 11a**). The blood AUC represents a total systemic exposure of the corresponding nanoparticle system. We selected the $AUC_{0-\infty}$ rather than the AUC_{0-t} to address the challenge that different studies used different end time points. We chose the non-compartmental model because it requires fewer assumptions than other models.^[244] We compiled 152 unique nanoparticle datasets from 82 papers to evaluate the nanoparticle pharmacokinetics in preclinical mouse models. We tabulated the physicochemical characteristics for each nanoparticle dataset to enable comparisons for different parameters (Material, Size, Shape, etc., **Figure 11b–j**).

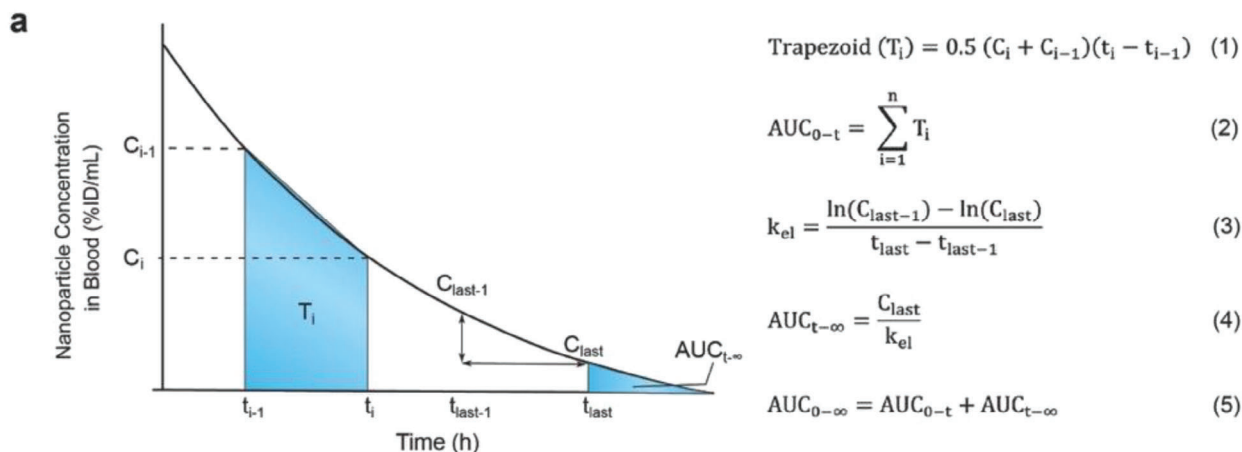
The median values and box positions in **Figure 11b–j** and **Table S6** (Supporting Information) revealed the following trends:

Table 1. List of factors and categories evaluated in the literature analysis.

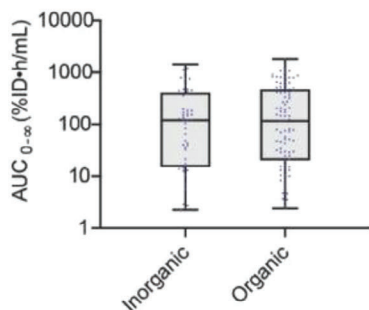
Factor	Category
Material	Inorganic, Organic
Material-inorganic	Gold, Iron oxide, Silica, Other-inorganic
Material-organic	Biological, Liposome, Polymeric, Other-organic
Hydrodynamic Diameter (nm)	≤ 10 , 11 – 100, 101 – 200, >200
Zeta Potential (mV)	Negative (<-10), Neutral (-10 to 10), Positive (>10)
Shape	Spherical, Rod, Other
PEG-containing	Yes, No
Surface Chemistry	Biological, Bio-PEG, Small molecule, SM-PEG, PEG, Other polymers
Animal Model	Healthy, Tumor

Abbreviations: Bio, biological; SM, small molecule.

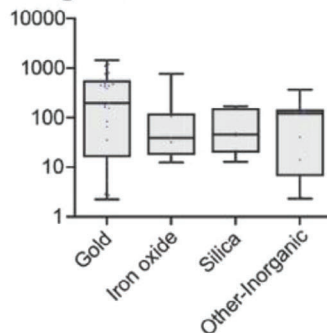
Material: The inorganic and organic materials exhibit comparable $AUC_{0-\infty}$ distributions, indicating a similar rate and extent of systemic circulation for nanoparticles from these two categories. Specifically for inorganic materials, gold nanoparticles, with the highest $AUC_{0-\infty}$ median of $196.5\%ID \cdot h/mL$, tend to undergo a higher exposure in the bloodstream than other inorganic compositions. Liposomes, with a median of $447.3\%ID \cdot h/mL$, exhibit the highest $AUC_{0-\infty}$ not only among the organic compositions (the medians of biological, polymeric, and other-organic categories are 46.2, 152.3, and $48.3\%ID \cdot h/mL$, respectively), but also the highest among all inorganic and organic categories, which indicates the highest total exposure in blood.



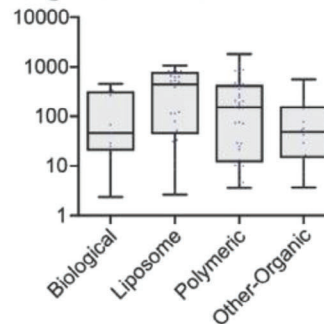
b Material



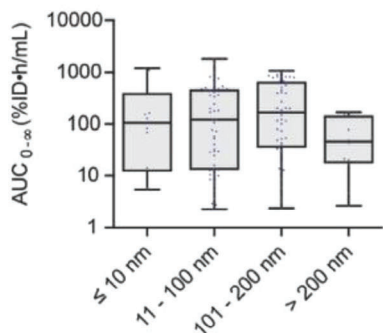
c Inorganic Material



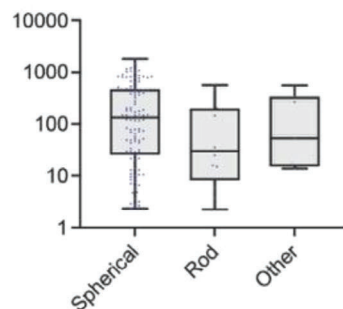
d Organic Material



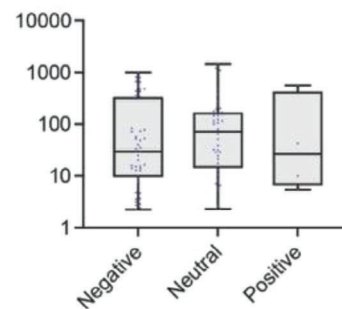
e Hydrodynamic Diameter



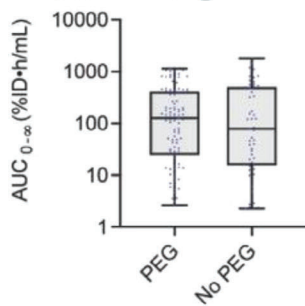
f Shape



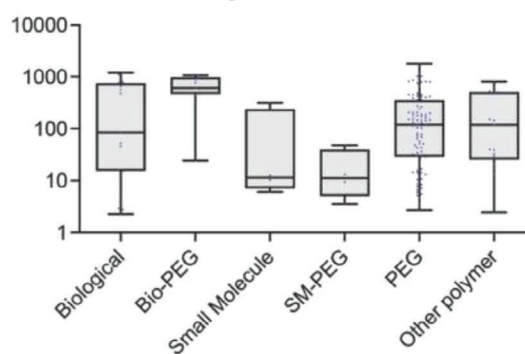
g Zeta Potential



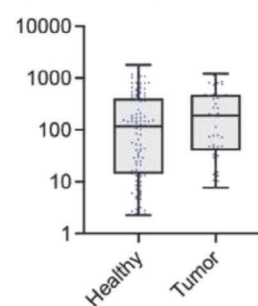
h PEG-Containing



i Surface Chemistry



j Animal Model



Zeta Potential: The zeta potential, estimating the surface charge of nanoparticles, does not noticeably affect the $AUC_{0-\infty}$ range, although the median of neutral nanoparticles is higher than positive and negative ones, which is consistent with what we observed in previously reported studies (see Section 4.4). However, when we assigned the nanoparticles with zwitterionic surface modification to a separate category, we observed a higher $AUC_{0-\infty}$ compared to other groups (Figure S1a and Table S6, Supporting Information). The median of the zwitterionic category is $1159.0\%ID\bullet h/mL$, while the ones of negative, neutral, and positive categories are $29.3\%ID\bullet h/mL$, $45.0\%ID\bullet h/mL$, and $26.4\%ID\bullet h/mL$, respectively. This trend indicates the potential of zwitterionic surface modification to maximize the pharmacokinetic properties of nanomedicines.

Surface Chemistry: When we organized the data into PEG-containing or not PEG-containing, we observed no significant increase in the $AUC_{0-\infty}$, although the median of the PEG-containing group is higher than the group without PEG. A probable reason is that the well-known circulation prolonging function of PEG is masked by being analyzed with other surface designs, such as targeting and camouflaging modifications. Therefore, we expanded the categories and differentiated between nanoparticles with surfaces modified with small molecules or biological coatings and nanoparticles with surfaces modified with PEG and small molecules or biological ligands (Small molecule vs SM-PEG; Biological vs Bio-PEG). With this expansion, although the small molecule and SM-PEG categories exhibit similar medians, the Bio-PEG category presents a higher $AUC_{0-\infty}$ median value than the biological category. Moreover, the Bio-PEG is the category with the highest $AUC_{0-\infty}$ median ($615.9\%ID\bullet h/mL$) among all surface chemistry categories (11.4 , 11.2 , 83.7 , 119.6 , and $119.8\%ID\bullet h/mL$ for small molecule, SM-PEG, biological, PEG, and other polymer, respectively).

We created a table that summarizes the categories of the highest and lowest $AUC_{0-\infty}$ medians under each factor as a reference for the nanomedicine field (Table 2). According to the table, nanoparticles comprised of gold or liposomes and with Bio-PEG surface chemistry demonstrate improved $AUC_{0-\infty}$. Further, nanoparticles with neutral surfaces and diameters ranging from 101–200 nm exhibit similarly favorable results. These parameters may be starting points when assessing nanoparticle formulations for increased total systemic exposure, prolonged blood circulation, and improved therapeutic performance.

The univariate and multivariate analyses were conducted to investigate the effect of each factor statistically (Section S2 and S3,

Table 2. Summary of physicochemical properties affecting nanoparticle pharmacokinetics.

Factor	Highest*	Lowest*
Material	Inorganic	Organic
Material-inorganic	Gold	Iron oxide
Material-organic	Liposome	Biological
Size (nm)	101–200	>200
Zeta Potential†	Neutral	Positive
Shape	Spherical	Rod
Surface Chemistry	Bio-PEG	SM-PEG

*Category of the highest or lowest $AUC_{0-\infty}$ median under each factor; †Neutral, zeta potential is from -10 to 10 mV; Positive, zeta potential is > 10 mV.

Supporting Information). The P-values from both analyses are summarized in Table 3. A lower P-value indicates a higher probability for the factor (covariable) to affect the outcome variable, which was log-transformed $AUC_{0-\infty}$ in this case.

Based on the univariate analysis, the parameter “Surface Chemistry” is significantly associated with log-transformed $AUC_{0-\infty}$ ($p = 0.005$). Although the P-values of Animal Model

Table 3. Effect factor P-values for nanoparticle blood circulation obtained from statistical analyses.

Blood	
Univariate Analysis	P-value*
Surface Chemistry	0.005
Animal Model	0.069
Material-all	0.080
Size	0.163
Shape	0.315
Zeta Potential	0.576
Material	0.577
PEG-containing	0.652
Multivariate Analysis	
	P-value
Animal Model	0.017
Surface Chemistry	0.078
Material-all	0.459

Log-transformation of $AUC_{0-\infty}$ was performed before analysis. *P-values based on the Kruskal-Wallis test.

Figure 11. Analysis of the nanoparticle pharmacokinetics in mice. a) The non-compartmental model used was the slope, height, area, and momentum (SHAM) model. This model was applied to calculate the area-under-the-curve from the zero point to infinity ($AUC_{0-\infty}$) of the plot of nanoparticle concentration in blood versus time. Equations (1–5) were used to calculate $AUC_{0-\infty}$, which is composed of two parts, AUC_{0-t} (AUC from zero to last time point; equations 1–2) and $AUC_{t-\infty}$ (AUC from last time point to infinity; equations 3–4). AUC_{0-t} was calculated by the linear trapezoidal method, in which T_i represents the area of the trapezoid between time $t_i - 1$ and t_i (equation 1), and AUC_{0-t} is obtained by summing up all trapezoid areas from $i = 1$ to $i = n$ (equation 2). $AUC_{t-\infty}$, the “triangle” at the end of the curve, was calculated using the terminal slope (k_{el} , elimination rate constant) and the nanoparticle concentration at the last time point (C_{last}). k_{el} was obtained based on the data of the last two time points, (C_{last} , t_{last}) and (C_{last-1} , t_{last-1}), according to equation 3. $AUC_{t-\infty}$ was then calculated by dividing C_{last} by k_{el} (equation 4). Finally, $AUC_{0-\infty}$ equals the summation of AUC_{0-t} and $AUC_{t-\infty}$ (equation 5). b–j) Categorical analysis of the blood $AUC_{0-\infty}$ data. The effects of factors were analyzed, including: b) Material, c) Inorganic Material composition, d) Organic Material composition, e) Hydrodynamic Diameter, f) Shape, g) Zeta Potential, h) PEG-containing condition, i) Surface Chemistry, and j) Animal Model. Individual data points and box-and-whisker plots are presented simultaneously. In the plots, a box represents the 25th to 75th percentile values, and the black solid line in the box indicates the median. The top and bottom lines indicate the maximum and minimum values.

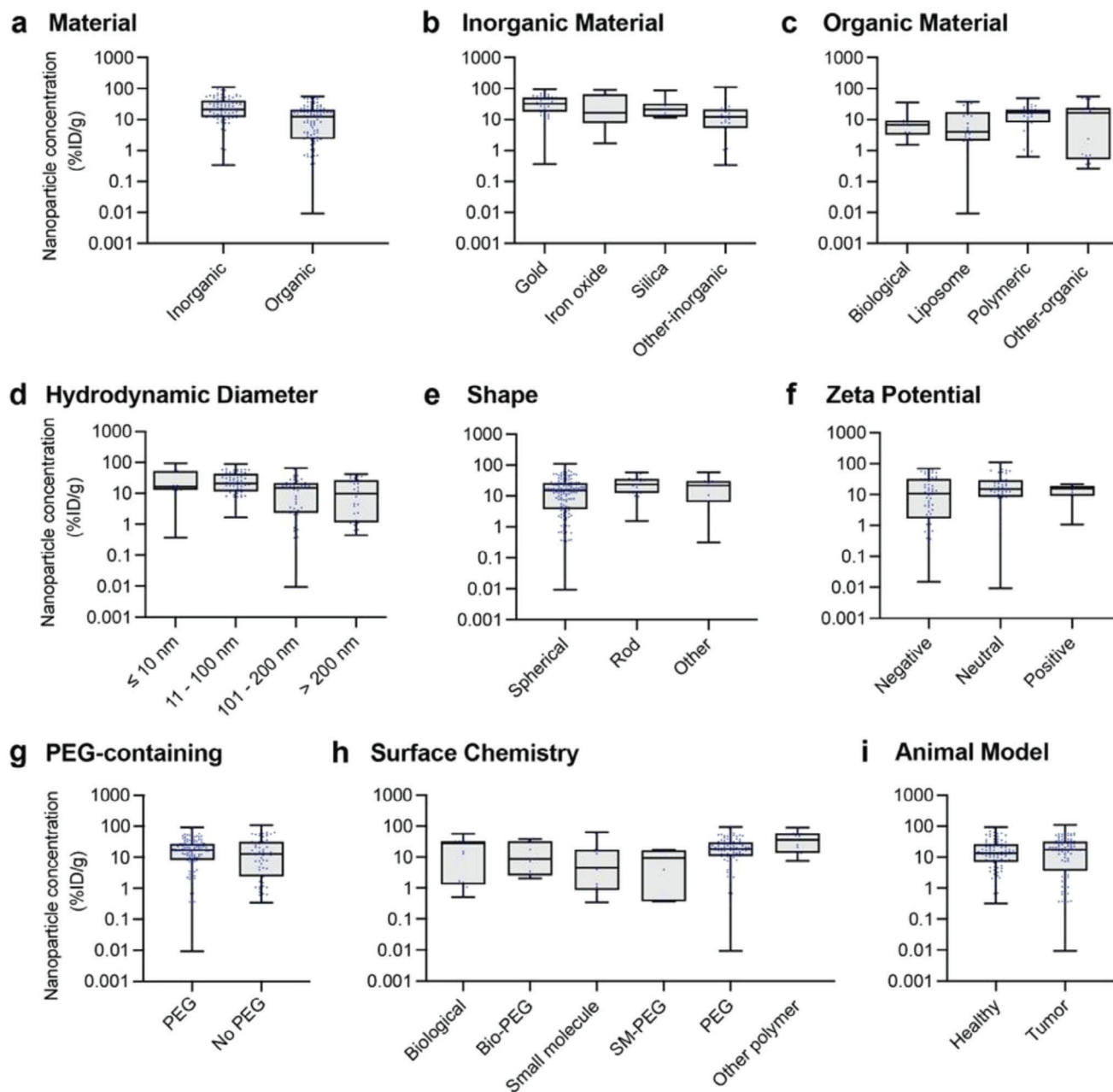


Figure 12. Categorical analysis of nanoparticle concentration data in the liver 24 h after systemic administration. The effects of factors were analyzed, including: a) Material, b) Inorganic Material composition, c) Organic Material composition, d) Hydrodynamic Diameter, e) Shape, f) Zeta Potential, g) PEG-containing condition, h) Surface Chemistry, and i) Animal Model. Individual data points and box-and-whisker plots are presented simultaneously. In the plots, a box represents the 25th to 75th percentile values, and the black solid line in the box indicates the median. The top and bottom lines indicate the maximum and minimum values.

and Material-all (combination of all categories from Material-inorganic and Material-organic) are larger than 0.05, they are small enough ($p < 0.15$) and were included in multivariate analysis. The multivariate analysis results showed the Animal Model as the most predictive factor ($p = 0.017$), followed by Surface Chemistry and Material-all. These results indicate three potential influencing factors on $AUC_{0-\infty}$: nanoparticle surface chemistry, nanoparticle material composition, and animal model. Physical properties, such as nanoparticle size and shape,

do not appear to significantly influence $AUC_{0-\infty}$ based on the analyzed data.

The nanoparticle number injection dose has recently been reported to affect nanoparticle pharmacokinetics and tumor delivery efficiency.^[65] However, only a limited number of studies reported this metric in our literature survey. To overcome this limitation and to enable an analysis of the injection dose metric, we recalculated the injected nanoparticle numbers of our compiled gold nanoparticle and liposome datasets because these

Table 4. Summary of physicochemical properties affecting nanoparticle organ biodistribution.

Category	Liver		Spleen		Lung		Kidney	
	Lowest*	Highest*	Lowest	Highest	Lowest	Highest	Lowest	Highest
Material	Organic	Inorganic	Organic	Inorganic	Organic	Inorganic	Organic	Inorganic
Material-inorganic	Other-inorganic	Gold	Other-inorganic	Silica	Other-inorganic	Iron oxide	Silica	Other-inorganic
Material-organic	Liposome	Polymeric	Biological	Polymeric	Biological	Polymeric	Other-organic	Polymeric
Size (nm)	>200	11-100	>200	101-200	>200	11-100	>200	<10
Zeta Potential [†]	Negative	Neutral	Positive	Neutral	Negative	Neutral	Negative	Neutral
Shape	Spherical	Rod	Spherical	Rod/Other	Spherical	Rod	Other	Rod
Surface Chemistry	Small molecule	Other polymer	Small molecule	Other polymer	Small molecule	Other polymer	Bio-PEG	SM-PEG

*Categories showing the lowest and highest nanoparticle concentration median at 24 h post-administration for each parameter in different organs. [†]Neutral, zeta potential is from -10 to 10 mV; Negative, zeta potential is < -10 mV; Positive, zeta potential is > 10 mV.

materials are frequently used inorganic and organic nanoparticles, respectively (Data S2, Supporting Information). The plot of the nanoparticle number injection dose versus $AUC_{0-\infty}$ indicates that, generally, a high injection dose tends to increase the $AUC_{0-\infty}$ (Figure S2, Supporting Information).

6.2. Nanoparticle Biodistribution

The liver, spleen, lung, and kidneys are major nanoparticle clearance organs. All compiled nanoparticle concentration data in these four organs (Data S1, Supporting Information), presented as %ID/g 24 h after nanoparticle administration, were summarized in Figure S3 (Supporting Information). The time point of 24 h was selected since most of the complied studies reported data for this time point. Overall, the liver and spleen exhibited higher nanoparticle retention than the lung and kidney at 24 h, which indicates the essential role of the liver and spleen over other organs for clearing systemically administered nanoparticles.

To further unravel how the design affects nanoparticle distribution and retention, the datasets of each organ were analyzed by the same categorical and statistical strategies used in the blood data analysis. The plots of the nanoparticle concentration data were summarized based on organs in **Figure 12** and Figures S4–S6 (Supporting Information) for the liver, spleen, lung, and kidney, respectively. The detailed nanoparticle concentration median in the unit %ID/g and the number of datasets of each analyzed category are listed in Table S7 (Supporting Information), while the corresponding information in the unit %ID is listed in Table S8 (Supporting Information). A lower nanoparticle concentration may suggest lower organ accumulation or longer blood circulation, while a higher concentration may suggest passive organ targeting, long tissue retention, or short blood circulation.^[245]

We provide a table recapitulating the categories with the lowest and highest median for each factor and organ (**Table 4**). The categories under the “lowest” column are preferred for a specific organ when lower accumulation is desired, while those under the “highest” column may facilitate organ targeting strategies. Therefore, before a new nanomedicine development, researchers may consider the nanoparticle in vivo mapping in advance, including the specific organ the nanoparticle is targeting and the organs the nanoparticle should avoid due to undesirable toxicity or elimina-

tion. After this critical assessment, the researchers may flexibly use the information from the table to design nanoparticle chemical and physical characteristics for desired biodistribution and performance.

To comprehensively understand the trends in nanoparticle biodistribution, the influence of each factor across four organs was compared and discussed.

Material: Overall, inorganic nanoparticles show noticeably higher accumulation or longer retention than organic ones in all four organs, especially the liver and spleen. Polymeric nanoparticles present the highest accumulation in all organs for organic compositions, while liposomes and biological nanoparticles are the lowest two categories for the liver, spleen, and lung. For inorganic compositions, the patterns are various among organs. Gold presents the highest median for the liver, while silica for the spleen, iron oxide for the lung, and other-inorganic for the kidney.

Size: Nanoparticles with hydrodynamic diameter ≤ 10 nm tend to accumulate in the kidney, likely due to the quick glomerular filtration process for small nanoparticles. In other organs, middle-sized nanoparticles ranging in the 11–100 nm or 101–200 nm categories present the highest accumulation. Large nanoparticles with diameters > 200 nm show the lowest accumulation for all four organs.

Zeta Potential: Nanoparticles with neutral surfaces tend to accumulate in all four organs. When nanoparticles with zwitterionic surface were isolated as a separate category, it became the highest category in the liver, lung, and kidney instead of neutral (Figure S1, Supporting Information).

Shape: Rod-shaped nanoparticles show the highest accumulation in all four studied organs.

We conducted univariate and multivariate statistical analyses for all four organs (**Table 5**; Tables S3–S5 and Sections S4–S7, Supporting Information). The results suggest that the binary Material classification, inorganic and organic, is enough to have an impact on nanoparticle accumulation and retention in the liver ($p < 0.001$, Table 5) and spleen ($p < 0.001$, Table S3, Supporting Information) at the 24 h time point. In addition, Material-all, Surface Chemistry, Shape, and Size, are all factors significantly associated with local nanoparticle concentration ($p < 0.05$) in the liver and spleen based on multivariate analysis. When it comes to

Table 5. Effect factor P-values for the nanoparticle concentration in the liver at 24 h obtained from statistical analyses.

Liver	
Univariate Analysis	P-value*
Material	< 0.001
Material-all	< 0.001
Size	< 0.001
Surface Chemistry	0.002
Shape	0.079
Zeta Potential	0.122
PEG-containing	0.350
Animal Model	0.794
Multivariate Analysis	
	P-value
Material-all	< 0.0001
Surface Chemistry	0.0083
Shape	0.0092
Size	0.0096

Box-Cox transformation was performed before analysis. *P values based on the ANOVA model.

the lung and kidney, no factor significantly influences nanoparticle accumulation based on the multivariate analysis. However, Material-all, Size, and Zeta Potential affect the outcome variable when using univariate analysis.

6.3. Interpreting Pharmacokinetics and Biodistribution Results

The blood circulation and biodistribution behaviors of nanoparticles are interconnected. Two parameters, “Material-all” and “Surface Chemistry”, stand out from others. In Table S9 (Supporting Information), which summarizes analyzed parameters of which P-values were <0.05 in each group, “Material-all” is shown to have $P < 0.05$ in 4 analyzed groups (liver, spleen, lung, and kidney) in the univariate analysis and in 2 groups (liver and spleen) in the multivariate analysis. Similarly, “Surface Chemistry” demonstrates $P < 0.05$ in three groups (blood, liver, and spleen) and two groups (liver and spleen) in the univariate and multivariate analysis, respectively. These results statistically confirmed the determinant effect of the two parameters.

Among all compositions, liposomes exhibit the highest $AUC_{0-\infty}$ over other organic and inorganic categories (276% increase compared to the median of all nanoparticles, Table S10, Supporting Information), indicating the best pharmacokinetic characteristic after systemic administration. The accumulation of liposomes in the investigated organs is relatively low. Bio-PEG is the most remarkable category relative to analyzed surface chemistries, which increased the $AUC_{0-\infty}$ median of modified nanoparticles by $\approx 418\%$ compared with all assessed nanoparticles (Table S10, Supporting Information). The PEG component provides stability and stealth effects to nanoparticles, while the biological component increases biocompatibility or provides specific biological functions. The biological components analyzed include peptides, proteins, antibodies, hyaluronic acid, and cell membranes. A majority of them functioned to pretend the coated

nanoparticles as non-foreign material. For example, the erythrocyte membrane coating with CD47 on the surface as a self-marker, camouflaged the nanoparticles from recognition by the NBRP.^[246,247] In another example, the functional fragment of CD47, “self-peptide”, was applied to the nanoparticle surface to signal “do not eat me” to phagocytic cells.^[248] Some endogenous molecules, such as serum albumin, were exploited to mitigate the opsonization and subsequent phagocytosis.^[249,250] The joint function of PEG and biological components improves the performance of the modified nanoparticles.

Beyond nanoparticle material and surface chemistry, we categorized nanoparticle systemic circulation and biodistribution according to the year the study was published to evaluate the progress in the field of nanomedicine (Figure S7 and Tables S6 and S7, Supporting Information). Obvious improvements in $AUC_{0-\infty}$ of nanoparticle systemic circulation with significantly decreasing organ accumulation (except for the kidneys) were achieved in the last two and half years (2019 – middle of 2021). For the blood $AUC_{0-\infty}$ parameter, the median value (142.3%ID•h/mL) of the timeframe from 2019 to 2021 increased $\approx 37\%$ when compared with that of 2011–2018 (103.8%ID•h/mL). While for the biodistribution, a decrease of 69%, 81%, and 39% was observed for the liver, spleen, and lung, respectively, by comparing median values of 2019–2021 to that of 2011–2018 (nanoparticle concentration in %ID/g: 5.6 vs 17.8 for the liver, 3.7 vs 19.2 for the spleen, and 1.3 vs 2.1 for the lung). Continued success in line with these trends will enhance the clinical translation of nanomedicines.

Through our literature survey, many valuable trends were observed and statistically analyzed, which may assist the understanding of nano-bio interactions. However, there are still limitations and shortcomings that should be addressed in future studies (see Section S8, Supporting Information).

7. Discussion

Efficient in vivo delivery is critical for safe and effective diagnostic and therapeutic applications of nanomedicines, which requires a thorough understanding of how nanoparticles interact with biological systems. However, the complex nano-bio interactions have not been completely elucidated. Papers detailing new nanoparticle formulations often focus primarily on new and improved targeting strategies and therapeutic efficacy. As a result, these studies are often limited and incomplete relative to the assessment and reporting of pharmacokinetics and biodistribution. While more efficient targeting is a significant need in the field, formulation studies should further consider biological interactions to be clinically relevant.^[9,10] More comprehensive pharmacokinetics and biodistribution studies for emerging nanoparticle formulations will be key in understanding the interactions of different materials, properties, and surface functionalities of nanoparticles with organs, tissues, and cell types in the body.

Based on our literature analysis, we propose to address several limitations in the field. First, standardizations of animal and pharmacokinetics model selection, experimental protocols, and data presentation are lacking. Most published studies reported results in isolation, providing limited information to enable comparisons between different works. To address this challenge, experimental design and data reporting guidelines should be

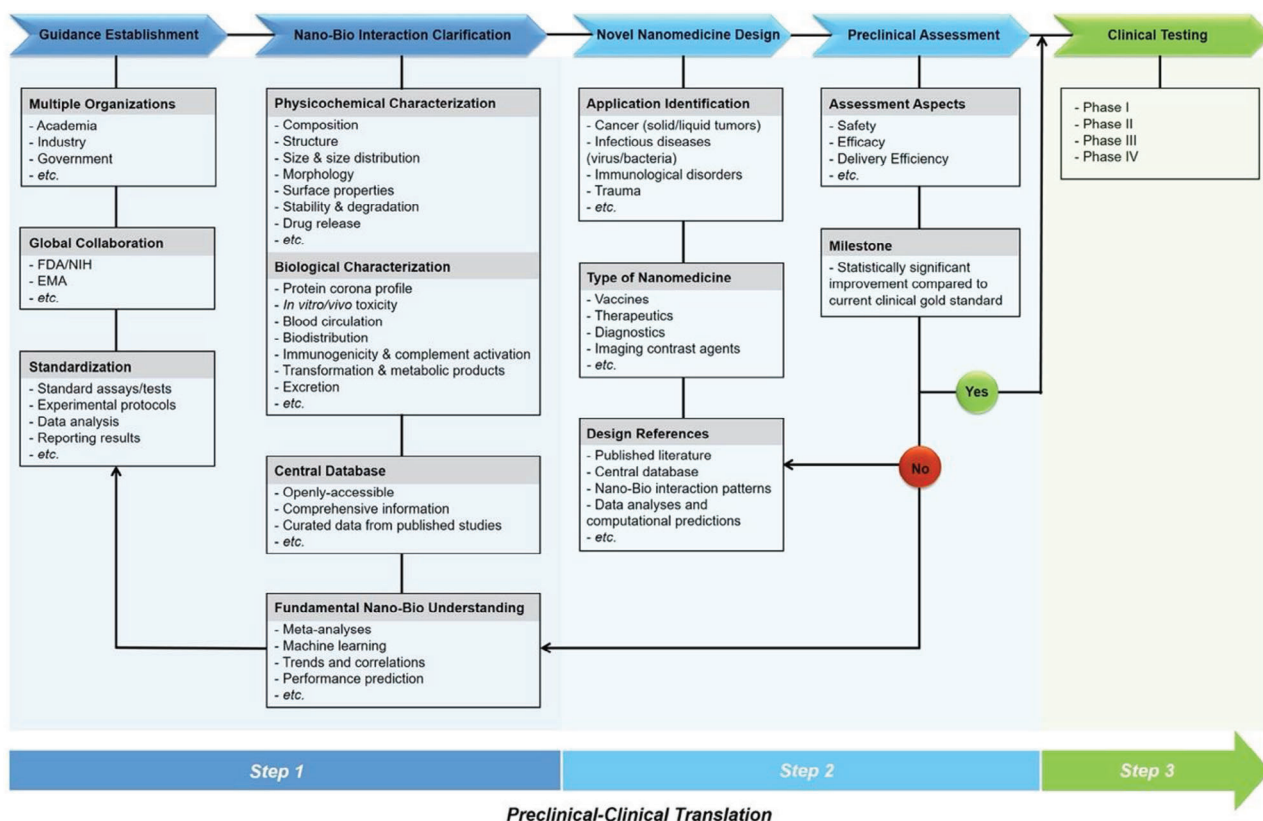


Figure 13. Proposed workflow to enhance nanomedicine translation. We propose a workflow to transform the understanding of nano-bio interactions and to advance progress in nanomedicine development and clinical application. PK, pharmacokinetics; BD, biodistribution.

established to improve communication and comparison surrounding pharmacokinetic and biodistribution studies. Additionally, we propose to provide experimental information, results, and data analysis in multiple ways. For example, the information about injection dose should be more comprehensive, including the number of nanoparticles, mass amount, loaded drug mass/molar amount, and radioactivity, among other similar quantification strategies. The plasma concentration versus time data should be analyzed using multiple pharmacokinetic models instead of only one, and as many pharmacokinetic parameters as feasible should be included in published studies. In biodistribution studies, the results of the quantitative analysis should be represented as %ID/g and additionally as %ID/organ to enhance relevance to overall biodistribution and potential for toxicity.

Second, the long-term studies of nanoparticle biodistribution are limited in the field. Most current studies only report the nanoparticle biodistribution data for up to one week. Extending biodistribution analysis to time points as long as weeks, months, and even years will help to characterize better the potential long-term adverse effects of nanomedicines. In addition, there is a lack of distinguishing between elimination and degradation; degradation of nanoparticles after administration was not addressed in most studies. Besides the elimination of nanoparticles from the body, the measured decrease of the nanoparticle concentration in the blood and organs may result from a) degradation or metabolism of the entire nanoparticle, or b) detachment of labeling molecules. Other researchers have also brought up similar

concerns.^[251] In addition, the analysis and consideration of the toxicity and fate of degradation products should be strengthened.

Third, the importance of the protein corona is underestimated. The protein corona is the “middleman” at the interface of nanoparticles and biological systems. It changes the original physicochemical and biological properties of nanoparticles and affects or even determines nanoparticle in vivo behaviors, including circulation, clearance, distribution, toxicity, and immune response. However, both the correlations of nanoparticle-protein corona and protein corona-biological response are still unclear. Further studies are needed to clarify the role of the protein corona and to characterize the dynamic changes occurring in vivo.

Biological barriers to efficient drug delivery using nanoparticles are complex and diverse. Such barriers comprise a wide range of organs and cell types and have evolved specifically to keep foreign matter like nanoparticles out of systemic circulation. The complexity and thoroughness of our body’s defenses are astounding, and even with decades of continuous refining of nanoparticle design, recent reviews have stated that “we are not quite there yet” when it comes to the engineering of efficient nanoparticle-based delivery systems.^[252]

8. Perspective

To comprehensively understand nano-bio interactions, we present a proposed flow chart in **Figure 13** that summarizes the

collaborative efforts necessary to advance nanomedicine research and clinical outcomes. We emphasize the importance of establishing a comprehensive and curated central database for nano-bio interaction datasets to enable the analysis of trends and correlations using machine learning (ML) and artificial intelligence (AI). These data analyses have the potential to inform the fundamental understanding of nano-bio interactions, which could guide the engineering of next-generation nanomedicines.

Standardization is a key factor in facilitating efficient data mining and systematic analyses. However, standardization should not limit scientific creativity. The MIRIBEL (Minimum Information Reporting in Bio-Nano Experimental Literature) initiative is an intriguing starting point that may be continuously refined to accommodate advancements in the field, such as protein corona characterization, the spatiotemporal imaging of nanoparticle distribution and delivery,^[203,253–258] and the dose threshold effect.^[259,65,260]

We suggest standard protocols for individual nanoparticle characterization assays, such as from the National Institutes of Health (NIH) National Cancer Institute's Nanotechnology Characterization Lab (NCI-NCL) (<https://ncl.cancer.gov/resources/assay-cascade-protocols>). The establishment of standards for quantitative protein corona analyses is needed. Many published protein corona studies were performed *in vitro*, where the serum source, serum concentration, incubation time, incubation temperature, and centrifuge conditions varied between studies, influencing the resultant protein corona compositions.^[261,262] Generally, *in vitro* assessments are limited in how they recapitulate *in vivo* conditions.^[260,263] Thus, we encourage more standardized *in vivo* investigation of the protein corona in future studies.

Further, establishing centralized, comprehensive, and up-to-date repositories with open access to compile, standardize, and categorize research data is indispensable. While several nanomedicine or nanomaterial databases have been established, such as caNanoLab (<https://cananolab.cancer.gov/#/>) by the NIH NCI, PubVINAS by the Zhu Research Group (<https://www.pubvinas.com/>), and eNanoMapper (<http://www.enanomapper.net/>) by eight European partners, expanding these efforts will facilitate progress in the field.^[264,265] In addition, the application of AI technology will enable data mining and subsequent analyses. Many studies have used AI approaches to compile data on nano-bio interactions and pharmacokinetics.^[266–272] Additionally, *in silico* model development and testing with continually advancing computer-based methods provides further opportunities for predicting nano-bio interactions.^[273–276] Meta-analyses and machine learning may entangle physicochemical and other variables to predict nanomedicine performance, enabling a better understanding of nano-bio interactions for nanoparticle delivery.^[6,9,262,277] The compiled datasets used in most meta-analyses in nanomedicine are manually extracted or adopted from previous similar work.^[278–283] The combination of curated up-to-date online databases, computer-based analysis, and AI data interpretation and prediction methods significantly improve the timescale for completing new meta-analyses relating nanoparticle characteristics with *in vivo* nano-bio interactions. Implementing these strategies will further inform directions for future nanoparticle engineering.

9. Conclusion

In this review, we first explored the nanoparticle blood removal pathways (NBRP). We then looked at strategies developed to overcome biological barriers to nano-delivery. The first group of these strategies is based on modulating the characteristics of the nanoparticle itself. The second group of these strategies focuses on modulating the biological environment of the NBRP. Our literature survey reported the effects of some of these strategies on nanoparticle pharmacokinetic performance and biodistribution patterns. Even though there are limitations, the results systematically analyzed and summarized the status of nano-bio interaction research in the last ten years and provided information to assist future nanomedicine development. Simultaneously, key opportunities for improvements in the field of nanomedicine are revealed. Specifically, the establishment of design and reporting standardization with central data repositories and the utilization of meta-analysis and machine-learning techniques will assist in a better understanding of nano-bio interactions to inform the development of next-generation nanomedicines.

Supporting Information

Supporting Information is available from the Wiley Online Library or from the author.

Acknowledgements

The authors thank Dr. B. Ouyang and G. Le for their helpful discussions. This work was supported in part by an NSF CAREER award (2048130), an NIH COBRE award (P20GM135009), an NIH MIRA R35 award (1R35GM150758), an IBEST/OUHSC seed grant for interdisciplinary research, the OU Faculty Investment Program, an OCAST Health Research grant (HR20-106), and the Oklahoma Tobacco Settlement Endowment Trust awarded to the University of Oklahoma – Stephenson Cancer Center. The content is solely the responsibility of the authors and does not necessarily represent the official views of the Oklahoma Tobacco Settlement Endowment Trust.

Conflict of Interest

The authors declare no conflict of interest.

Author Contributions

L.W. and S.Q. contributed equally to the work. L.W., S.Q., M.L., M.D.B., L.G.C., Y.D.Z., and S.W. contributed to the literature research and data analysis. All authors contributed to the writing and editing of the manuscript.

Keywords

biodistribution, biological barriers, literature survey, mononuclear phagocyte system, nano-bio interaction, nanomedicine, nanoparticle blood removal pathways, nanoparticle delivery, pharmacokinetics, reticuloendothelial system (RES)

Received: July 20, 2023

Revised: October 9, 2023

Published online:

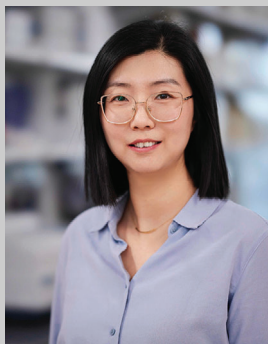
- [1] B. Pelaz, C. Alexiou, R. A. Alvarez-Puebla, F. Alves, A. M. Andrews, S. Ashraf, L. P. Balogh, L. Ballerini, A. Bestetti, C. Brendel, S. Bosi, M. Carril, W. C. W. Chan, C. Chen, X. Chen, X. Chen, Z. Cheng, D. Cui, J. Du, C. Dullin, A. Escudero, N. Feliu, M. Gao, M. George, Y. Gogotsi, A. Grünweller, Z. Gu, N. J. Halas, N. Hampp, R. K. Hartmann, et al., *ACS Nano* **2017**, *11*, 2313.
- [2] Q. Dai, S. Wilhelm, D. Ding, A. M. Syed, S. Sindhvani, Y. W. Zhang, Y. Y. Chen, P. MacMillan, W. C. W. Chan, *ACS Nano* **2018**, *12*, 8423.
- [3] F. Danhier, *J. Controlled Release* **2016**, *244*, 108.
- [4] Y.-N. Zhang, W. Poon, A. J. Tavares, I. D. McGilvray, W. C. W. Chan, *J. Controlled Release* **2016**, *240*, 332.
- [5] S. Wilhelm, A. J. Tavares, W. C. W. Chan, *Nat. Rev. Mater.* **2016**, *1*, 16074.
- [6] S. Wilhelm, A. J. Tavares, Q. Dai, S. Ohta, J. Audet, H. F. Dvorak, W. C. W. Chan, *Nat. Rev. Mater.* **2016**, *1*, 16014.
- [7] Z. Zhao, A. Ukidve, J. Kim, S. Mitragotri, *Cell* **2020**, *181*, 151.
- [8] M. J. Mitchell, M. M. Billingsley, R. M. Haley, M. E. Wechsler, N. A. Peppas, R. Langer, *Nat. Rev. Drug Discovery* **2021**, *20*, 101.
- [9] W. Poon, B. R. Kingston, B. Ouyang, W. Ngo, W. C. W. Chan, *Nat. Nanotechnol.* **2020**, *15*, 819.
- [10] E. Blanco, H. Shen, M. Ferrari, *Nat. Biotechnol.* **2015**, *33*, 941.
- [11] Part of the Content and Several Figures in This Article are Adopted from Skyler Quine's Master Thesis. Uri: <https://hdl.handle.net/11244/324416>
- [12] S. D. Li, L. Huang, *Mol. Pharmaceutics* **2008**, *5*, 496.
- [13] M. G. Lu, K. T. Al-Jamal, K. Kostarelos, J. Reineke, *ACS Nano* **2010**, *4*, 6303.
- [14] K. Sugano, M. Kansy, P. Artursson, A. Avdeef, S. Bendels, L. Di, G. F. Ecker, B. Faller, H. Fischer, G. Gerebtzoff, H. Lennernaes, F. Senner, *Nat. Rev. Drug Discovery* **2010**, *9*, 597.
- [15] A. M. Vargason, A. C. Anselmo, S. Mitragotri, *Nat. Biomed. Eng.* **2021**, *5*, 951.
- [16] N. Hoshyar, S. Gray, H. B. Han, G. Bao, *Nanomedicine* **2016**, *11*, 673.
- [17] D. F. Yuan, H. He, Y. Wu, J. H. Fan, Y. G. Cao, *J. Pharm. Sci.* **2019**, *108*, 58.
- [18] D. Sarker, *Curr. Drug Delivery* **2005**, *2*, 297.
- [19] K. W. Kang, M. G. Song, in *Radionanomedicine: Combined Nuclear and Nanomedicine*, (Ed: D. S. Lee), Springer, Cham **2018**, pp. 105–123.
- [20] S. Luo, J. Ding, P. Wang, Z. Wang, X. Ma, C. Yang, Q. Liang, P. Rong, W. Wang, *Contrast Media Mol. Imaging* **2018**, *2018*, 2957459.
- [21] C. Halma, M. R. Daha, L. A. Es, *Clin. Exp. Immunol.* **1992**, *89*, 1.
- [22] C. L. Anderson, *J. Leukoc. Biol.* **2015**, *98*, 875.
- [23] K. Wake, Y. Kawai, B. Smedsrød, *Ital. J. Anat. Embryol.* **2001**, *106*, 261.
- [24] L. Aschoff, in *Ergebnisse Der Inneren Medizin Und Kinderheilkunde*, (Eds: F. Kraus, E. Meyer, O. Minkowski, Fr. Müller, H. Sahli, A. Schittenhelm, A. Czerny, O. Heubner, L. Langstein), Springer, Berlin, Heidelberg **1924**, p. 1.
- [25] R. v. Furth, Z. A. Cohn, J. G. Hirsch, J. H. Humphrey, W. G. Spector, H. L. Langevoort, *Bull. World Health Organ.* **1972**, *46*, 845.
- [26] S. Yona, S. Gordon, *Front. Immunol.* **2015**, *6*, 328.
- [27] Y. Kawai, B. Smedsrød, K. Elvevold, K. Wake, *Cell Tissue Res.* **1998**, *292*, 395.
- [28] B. Smedsrød, H. Pertoft, S. Gustafson, T. C. Laurent, *Biochem. J.* **1990**, *266*, 313.
- [29] F. Campbell, F. L. Bos, S. Sieber, G. Arias-Alpizar, B. E. Koch, J. Huwyler, A. Kros, J. Bussmann, *ACS Nano* **2018**, *12*, 2138.
- [30] Y. Tang, X. Wang, J. Li, Y. Nie, G. Liao, Y. Yu, C. Li, *ACS Nano* **2019**, *13*, 13015.
- [31] S. Z. Chong, M. Evrard, C. C. Goh, L. G. Ng, *Curr. Opin. Immunol.* **2018**, *50*, 94.
- [32] M. Williams, F. Ginhoux, C. Jakubzick, S. H. Naik, N. Onai, B. U. Schraml, E. Segura, R. Tussiwand, S. Yona, *Nat. Rev. Immunol.* **2014**, *14*, 571.
- [33] U. S. Gaharwar, R. Meena, P. Rajamani, *J. Appl. Toxicol.* **2017**, *37*, 1232.
- [34] Y. Wu, W. Wu, W. M. Wong, E. Ward, A. J. Thrasher, D. Goldblatt, M. Osman, P. Digard, D. H. Canaday, K. Gustafsson, *J. Immunol.* **2009**, *183*, 5622.
- [35] M. Mahmoudi, N. Bertrand, H. Zope, O. C. Farokhzad, *Nano Today* **2016**, *11*, 817.
- [36] J. Lazarovits, Y. Y. Chen, E. A. Sykes, W. C. W. Chan, *Chem. Commun.* **2015**, *51*, 2756.
- [37] Y. Zhang, J. L. Y. Wu, J. Lazarovits, W. C. W. Chan, *J. Am. Chem. Soc.* **2020**, *142*, 8827.
- [38] J. Lazarovits, Y. Y. Chen, F. Y. Song, W. N. Ngo, A. J. Tavares, Y. N. Zhang, J. Audet, B. Tang, Q. C. Lin, M. C. Tleugabulova, S. Wilhelm, J. R. Krieger, T. Mallevaey, W. C. W. Chan, **2019**, *Nano Lett.* *19*, 116.
- [39] Q. Xiao, M. Zoulikha, M. Qiu, C. Teng, C. Lin, X. Li, M. A. Sallam, Q. Xu, W. He, *Adv. Drug Delivery Rev.* **2022**, *186*, 114356.
- [40] D. E. Owens, N. A. Peppas, *Int. J. Pharm.* **2006**, *307*, 93.
- [41] S. M. Ahsan, C. M. Rao, M. F. Ahmad, *Adv. Exp. Med. Biol.* **2018**, *1048*, 175.
- [42] I. Hamad, O. Al-Hanbali, A. C. Hunter, K. J. Rutt, T. L. Andresen, S. M. Moghimi, *ACS Nano* **2010**, *4*, 6629.
- [43] R. Tavano, L. Gabrielli, E. Lubian, C. Fedeli, S. Visentin, P. P. D. Laureto, G. Arrigoni, A. Geffner-Smith, F. Chen, D. Simberg, G. Morgese, E. M. Benetti, L. Wu, S. M. Moghimi, F. Mancin, E. Papini, *ACS Nano* **2018**, *12*, 5834.
- [44] F. Chen, G. Wang, J. I. Griffin, B. Breneman, N. K. Banda, V. M. Holers, D. S. Backos, L. Wu, S. M. Moghimi, D. Simberg, *Nat. Nanotechnol.* **2017**, *12*, 387.
- [45] V. Sheth, L. Wang, R. Bhattacharya, P. Mukherjee, S. Wilhelm, *Adv. Funct. Mater.* **2021**, *31*, 2007363.
- [46] N. D. Donahue, H. Acar, S. Wilhelm, *Adv. Drug Delivery Rev.* **2019**, *143*, 68.
- [47] M. A. Dobrovolskaia, P. Aggarwal, J. B. Hall, S. E. McNeil, *Mol. Pharmaceutics* **2008**, *5*, 487.
- [48] J. L. Betker, D. Jones, C. R. Childs, K. M. Helm, K. Terrell, M. A. Nagel, T. J. Anchordoquy, *J. Controlled Release* **2018**, *286*, 85.
- [49] M. E. Lobatto, T. Binderup, P. M. Robson, L. F. P. Giesen, C. Calcagno, J. Witjes, F. Fay, S. Baxter, C. H. Wessel, M. Eldib, J. Bini, S. D. Carlin, E. S. G. Stroes, G. Storm, A. Kjaer, J. S. Lewis, T. Reiner, Z. A. Fayad, W. J. M. Mulder, C. Pérez-Medina, *Bioconjugate Chem.* **2019**, *31*, 360.
- [50] Y. Zhao, X. Sun, G. Zhang, B. G. Trewyn, I. I. Slowing, V. S. Y. Lin, *ACS Nano* **2011**, *5*, 1366.
- [51] T. Wang, J. Bai, X. Jiang, G. U. Nienhaus, *ACS Nano* **2012**, *6*, 1251.
- [52] Z. M. Zhao, A. Ukidve, V. Krishnan, A. Fehnel, D. C. Pan, Y. S. Gao, J. Kim, M. A. Evans, A. Mandal, J. L. Guo, V. R. Muzykantov, S. Mitragotri, *Nat. Biomed. Eng.* **2021**, *5*, 441.
- [53] E. Chambers, S. Mitragotri, *Exp. Biol. Med.* **2007**, *232*, 958.
- [54] J. S. Brenner, D. C. Pan, J. W. Myerson, O. A. Marcos-Contreras, C. H. Villa, P. Patel, H. Hekierski, S. Chatterjee, J. Q. Tao, H. Parhiz, K. Bhamidipati, T. G. Uhler, E. D. Hood, R. Y. Kiseleva, V. S. Shuvaev, T. Shuvaeva, M. Khoshnejad, I. Johnston, J. V. Gregory, J. Lahann, T. Wang, E. Cantu, W. M. Armstead, S. Mitragotri, V. Muzykantov, *Nat. Commun.* **2018**, *9*, 2684.
- [55] A. C. Anselmo, V. Gupta, B. J. Zern, D. Pan, M. Zakrewsky, V. Muzykantov, S. Mitragotri, *ACS Nano* **2013**, *7*, 11129.
- [56] Y.-W. Yang, W.-H. Luo, *J. Controlled Release* **2016**, *227*, 82.
- [57] N. Bertrand, J. C. Leroux, *J. Controlled Release* **2012**, *161*, 152.
- [58] F. K. Swirski, M. Nahrendorf, *Nat. Rev. Immunol.* **2018**, *18*, 733.
- [59] D. J. Lundy, K. H. Chen, E. K. W. Toh, P. C. H. Hsieh, *Sci. Rep.* **2016**, *6*, 25613.

- [60] K. Nagaoka, T. Matoba, Y. J. Mao, Y. Nakano, G. Ikeda, S. Egusa, M. Tokutome, R. Nagahama, K. Nakano, K. Sunagawa, K. Egashira, *PLoS One* **2015**, *10*, 0132451.
- [61] M. Tokutome, T. Matoba, Y. Nakano, A. Okahara, M. Fujiwara, J. I. Koga, K. Nakano, H. Tsutsui, K. Egashira, *Cardiovasc. Res.* **2019**, *115*, 419.
- [62] I. M. Dauber, K. M. Vanbenthuyzen, I. F. Mcmurtry, G. S. Wheeler, E. J. Lesnefsky, L. D. Horwitz, J. V. Weil, *Circ. Res.* **1990**, *66*, 986.
- [63] W. Ngo, S. Ahmed, C. Blackadar, B. Bussin, Q. Ji, S. M. Mladjenovic, Z. Sepahi, W. C. W. Chan, *Adv. Drug Delivery Rev.* **2022**, *185*, 114238.
- [64] S. H. Lee, P. M. Starkey, S. Gordon, *J. Exp. Med.* **1985**, *161*, 475.
- [65] B. Ouyang, W. Poon, Y. N. Zhang, Z. P. Lin, B. R. Kingston, A. J. Tavares, Y. W. Zhang, J. Chen, M. S. Valic, A. M. Syed, P. MacMillan, J. Couture-Senecal, G. Zheng, W. C. W. Chan, *Nat. Mater.* **2020**, *19*, 1362.
- [66] K. M. Tsoi, S. A. MacParland, X.-Z. Ma, V. N. Spetzler, J. Echeverri, B. Ouyang, S. M. Fadel, E. A. Sykes, N. Goldaracena, J. M. Kathis, J. B. Conneely, B. A. Alman, M. Selzner, M. A. Ostrowski, O. A. Adeyi, A. Zilman, I. D. McGilvray, W. C. W. Chan, *Nat. Mater.* **2016**, *15*, 1212.
- [67] C. Eipel, K. Abshagen, B. Vollmar, *World J. Gastroenterol.* **2010**, *16*, 6046.
- [68] E. Samuelsson, H. Shen, E. Blanco, M. Ferrari, J. Wolfram, *Colloids Surf., B* **2017**, *158*, 356.
- [69] A. Chadburn, *Semin. Hematol.* **2000**, *37*, 13.
- [70] R. E. Mebius, G. Kraal, *Nat. Rev. Immunol.* **2005**, *5*, 606.
- [71] M. F. Cesta, *Toxicol. Pathol.* **2006**, *34*, 455.
- [72] T. I. Arnon, R. M. Horton, I. L. Grigороva, J. G. Cyster, *Nature* **2013**, *493*, 684.
- [73] M. Demoy, J.-P. Andreux, C. Weingarten, B. Gouritin, V. Guilloux, P. Couvreur, *harm. Res.* **1999**, *16*, 37.
- [74] S. M. Moghimi, C. J. H. Porter, I. S. Muir, L. Illum, S. S. Davis, *Biochem. Biophys. Res. Commun.* **1991**, *177*, 861.
- [75] L. Zhang, Z. Cao, Y. Li, J.-R. Ella-Menye, T. Bai, S. Jiang, *ACS Nano* **2012**, *6*, 6681.
- [76] M. G. Levitzky, *Pulmonary Physiology*, 8 ed., McGraw-Hill Education, New York **2013**.
- [77] M. Belenkovich, J. Sznitman, N. Korin, *J. Biomech.* **2022**, *137*, 111082.
- [78] M. Paranjpe, C. C. Muller-Goymann, *Int. J. Mol. Sci.* **2014**, *15*, 5852.
- [79] E. Granton, J. H. Kim, J. Podstawka, B. G. Yipp, *Trends Immunol.* **2018**, *39*, 890.
- [80] B. G. Yipp, J. H. Kim, R. Lima, L. D. Zbytniuk, B. Petri, N. Swanlund, M. Ho, V. G. Szeto, T. Tak, L. Koenderman, P. Pickkers, A. T. J. Tool, T. W. Kuijpers, T. K. van den Berg, M. R. Looney, M. F. Krummel, P. Kubes, *Sci. Immunol.* **2017**, *2*, eaam8929.
- [81] D. F. Chu, J. Gao, Z. J. Wang, *ACS Nano* **2015**, *9*, 11800.
- [82] J. C. Kaczmarek, K. J. Kauffman, O. S. Fenton, K. Sadler, A. K. Patel, M. W. Heartlein, F. DeRosa, D. G. Anderson, *Nano Lett.* **2018**, *18*, 6449.
- [83] I. A. Khalil, M. A. Younis, S. Kimura, H. Harashima, *Biol. Pharm. Bull.* **2020**, *43*, 584.
- [84] J. C. Kaczmarek, A. K. Patel, L. H. Rhym, U. C. Palmiero, B. Bhat, M. W. Heartlein, F. DeRosa, D. G. Anderson, *Biomaterials* **2021**, *275*, 120966.
- [85] K. Muller, D. A. Fedosov, G. Gompper, *Sci. Rep.* **2014**, *4*, 4871.
- [86] G. Hu, J. W. Christman, *Front. Immunol.* **2019**, *10*, 2275.
- [87] N. Joshi, J. M. Walter, A. V. Misharin, *Cell. Immunol.* **2018**, *330*, 86.
- [88] S. Santiwarakool, H. Akita, I. A. Khalil, M. M. Abd Elwakil, Y. Sato, K. Kusumoto, H. Harashima, *J. Controlled Release* **2019**, *307*, 55.
- [89] Z. C. Deng, G. T. Kalin, D. L. Shi, V. V. Kalinichenko, *Am. J. Respir. Cell Mol. Biol.* **2021**, *64*, 292.
- [90] Q. Cheng, T. Wei, L. Farbiak, L. T. Johnson, S. A. Dilliard, D. J. Siegwart, *Nat. Nanotechnol.* **2020**, *15*, 313.
- [91] A. W. Dunn, V. V. Kalinichenko, D. L. Shi, *Adv. Healthcare Mater.* **2018**, *7*, 1800876.
- [92] J. F. Han, Q. Wang, Z. R. Zhang, T. Gong, X. Sun, *Small* **2014**, *10*, 524.
- [93] J. C. Kaczmarek, A. K. Patel, K. J. Kauffman, O. S. Fenton, M. J. Webber, M. W. Heartlein, F. DeRosa, D. G. Anderson, *Angew. Chem., Int. Ed.* **2016**, *55*, 13808.
- [94] S. Y. Lee, E. Jung, J. H. Park, J. W. Park, C. K. Shim, D. D. Kim, I. S. Yoon, H. J. Cho, *J. Colloid Interface Sci.* **2016**, *480*, 102.
- [95] G. S. Travlos, *Toxicol. Pathol.* **2006**, *34*, 548.
- [96] K. Kaushansky, M. A. Lichtman, J. T. Prchal, M. M. Levi, O. W. Press, L. J. Burns, M. Caligiuri, *Williams Hematology*, 9 ed., McGraw-Hill Education, New York **2016**.
- [97] M. Hassanshahi, A. Hassanshahi, S. Khabbazi, Y. W. Su, C. J. Xian, *Angiogenesis* **2017**, *20*, 427.
- [98] S. M. Moghimi, *Adv. Drug Delivery Rev.* **1995**, *17*, 61.
- [99] Y. Gottlieb, O. Topaz, L. A. Cohen, L. D. Yakov, T. Haber, A. Morgenstern, A. Weiss, K. C. Berman, E. Fibach, E. G. Meyron-Holtz, *Haematologica* **2012**, *97*, 994.
- [100] C. J. H. Porter, S. M. Moghimi, L. Illum, S. S. Davis, *FEBS Lett.* **1992**, *305*, 62.
- [101] Y.-W. Yang, W.-H. Luo, *Sci. Rep.* **2017**, *7*, 44691.
- [102] K. A. Walters, M. S. Roberts, *Dermatological and Transdermal Formulations*, CRC Press, Boca Raton, FL **2002**.
- [103] R. Kumar, I. Roy, T. Y. Ohulchanskyy, L. A. Vathy, E. J. Bergey, M. Sajjad, P. N. Prasad, *ACS Nano* **2010**, *4*, 699.
- [104] R. S. H. Yang, L. W. Chang, J.-P. Wu, M.-H. Tsai, H.-J. Wang, Y.-C. Kuo, T.-K. Yeh, C. S. Yang, P. Lin, *Environ. Health Perspect.* **2007**, *115*, 1339.
- [105] Y. Akiyama, T. Mori, Y. Katayama, T. Niidome, *J. Controlled Release* **2009**, *139*, 81.
- [106] E. A. Sykes, Q. Dai, K. M. Tsoi, D. M. Hwang, W. C. W. Chan, *Nat. Commun.* **2014**, *5*, 3796.
- [107] E. E. Gray, J. G. Cyster, *J. Innate Immun.* **2012**, *4*, 424.
- [108] Y.-N. Zhang, J. Lazarovits, W. Poon, B. Ouyang, L. N. M. Nguyen, B. R. Kingston, W. C. W. Chan, *Nano Lett.* **2019**, *19*, 7226.
- [109] F. Réty, O. Clément, N. Siauve, C. A. Cuénon, F. Carnot, M. Sich, A. Buisine, G. Frija, *J. Magn. Reson. Imaging* **2000**, *12*, 734.
- [110] M. J. Ernsting, M. Murakami, A. Roy, S.-D. Li, *J. Controlled Release* **2013**, *172*, 782.
- [111] P. P. Wyss, S. Lamichhane, A. Abed, D. Vonwil, O. Kretz, T. B. Huber, M. Sarem, V. P. Shastri, *Biomaterials* **2020**, *230*, 119643.
- [112] B. Du, M. Yu, J. Zheng, *Nat. Rev. Mater.* **2018**, *3*, 358.
- [113] R. Weissleder, M. J. Pittet, *Nat. Biomed. Eng.* **2020**, *4*, 489.
- [114] D. D. Castellì, E. Terreno, C. Cabella, L. Chaabane, S. Lanzardo, L. Tei, M. Visigalli, S. Aime, *NMR Biomed.* **2009**, *22*, 1084.
- [115] Y. Y. Huai, M. N. Hossen, S. Wilhelm, R. Bhattacharya, P. Mukherjee, *Bioconjugate Chem.* **2019**, *30*, 2247.
- [116] I. J. Fidler, *Adv. Drug Delivery Rev.* **1988**, *2*, 69.
- [117] F. Ahsan, I. P. Rivas, M. A. Khan, A. I. T. Suárez, *J. Controlled Release* **2002**, *79*, 29.
- [118] H. L. Ye, Z. Q. Shen, L. Yu, M. Wei, Y. Li, *Proc. R. Soc. A* **2018**, *474*, 20170845.
- [119] Z. Zhao, A. Ukidve, V. Krishnan, S. Mitragotri, *Adv. Drug Delivery Rev.* **2019**, *143*, 3.
- [120] V. Francia, D. Montizaan, A. Salvati, *Beilstein J. Nanotechnol.* **2020**, *11*, 338.
- [121] H. S. Leong, K. S. Butler, C. J. Brinker, M. Azzawi, S. Conlan, C. Dufes, A. Owen, S. Rannard, C. Scott, C. Y. Chen, M. A. Dobrovolskaia, S. V. Kozlov, A. Prina-Mello, R. Schmid, P. Wick, F. Caputo, P. Boisseau, R. M. Crist, S. E. McNeil, B. Fadeel, L. Tran, S. F. Hansen, N. B. Hartmann, L. P. W. Clausen, L. M. Skjolding, A. Baun, M. Ågerstrand, Z. Gu, D. A. Lamprou, C. Hoskins, et al., *Nat. Nanotechnol.* **2019**, *14*, 629.

- [122] G. Oberdörster, A. Maynard, K. Donaldson, V. Castranova, J. Fitzpatrick, K. Ausman, J. Carter, B. Karn, W. Kreyling, D. Lai, S. Olin, N. Monteiro-Riviere, D. Warheit, H. Yang, *Part. Fibre Toxicol.* **2005**, *2*, 8.
- [123] A. R. Gliga, S. Skoglund, I. O. Wallinder, B. Fadeel, H. L. Karlsson, *Part. Fibre Toxicol.* **2014**, *11*, 11.
- [124] A. Albanese, P. S. Tang, W. C. W. Chan, *Annu. Rev. Biomed. Eng.* **2012**, *14*, 1.
- [125] W. Yang, L. Wang, E. M. Mettenbrink, P. L. DeAngelis, S. Wilhelm, *N. Toxicology, Annu. Rev. Pharmacol. Toxicol.* **2021**, *61*, 269.
- [126] J. Lim, S. P. Yeap, H. X. Che, S. C. Low, *Nanoscale Res. Lett.* **2013**, *8*, 381.
- [127] Y. Wei, L. Quan, C. Zhou, Q. Zhan, *Nanomedicine* **2018**, *13*, 1495.
- [128] M. V. Baranov, M. Kumar, S. Sacanna, S. Thutupalli, G. van den Bogaart, *Front. Immunol.* **2021**, *11*, 607945.
- [129] X. J. Cheng, X. Tian, A. Q. Wu, J. X. Li, J. Tian, Y. Chong, Z. F. Chai, Y. L. Zhao, C. Y. Chen, C. C. Ge, *ACS Appl. Mater. Interfaces* **2015**, *7*, 20568.
- [130] C. D. Walkey, J. B. Olsen, H. B. Guo, A. Emili, W. C. W. Chan, *J. Am. Chem. Soc.* **2012**, *134*, 2139.
- [131] L. Leclerc, W. Rima, D. Boudard, J. Pourchez, V. Forest, V. Bin, P. Mowat, P. Perriat, O. Tillement, P. Grosseau, D. Bernache-Assollant, M. Cottier, *Inhalation Toxicol.* **2012**, *24*, 580.
- [132] M. S. de Almeida, E. Susnik, B. Drasler, P. Taladriz-Blanco, A. Petri-Fink, B. Rothen-Rutishauser, *Chem. Soc. Rev.* **2021**, *50*, 5397.
- [133] H. S. Choi, W. Liu, P. Misra, E. Tanaka, J. P. Zimmer, B. I. Ipe, M. G. Bawendi, J. V. Frangioni, *Nat. Biotechnol.* **2007**, *25*, 1165.
- [134] W. H. D. Jong, W. I. Hagens, P. Krystek, M. C. Burger, A. J. A. M. Sips, R. E. Geertsma, *Biomaterials* **2008**, *29*, 1912.
- [135] X. Li, Z. Hu, J. Ma, X. Wang, Y. Zhang, W. Wang, Z. Yuan, *Colloids Surf., B* **2018**, *167*, 260.
- [136] H. K. Mandl, E. Quijano, H. W. Suh, E. Sparago, S. Oeck, M. Grun, P. M. Glazer, W. M. Saltzman, *J. Controlled Release* **2019**, *314*, 92.
- [137] C. He, Y. Hu, L. Yin, C. Tang, C. Yin, *Biomaterials* **2010**, *31*, 3657.
- [138] E. Vlashi, L. E. Kelderhouse, J. E. Sturgis, P. S. Low, *ACS Nano* **2013**, *7*, 8573.
- [139] N. P. Truong, M. R. Whittaker, C. W. Mak, T. P. Davis, *Expert Opin. Drug Delivery* **2014**, *12*, 129.
- [140] N. Kapate, J. R. Clegg, S. Mitragotri, *Adv. Drug Delivery Rev.* **2021**, *177*, 113807.
- [141] C. Kinnear, T. L. Moore, L. Rodriguez-Lorenzo, B. Rothen-Rutishauser, A. Petri-Fink, *Chem. Rev.* **2017**, *117*, 11476.
- [142] R. Mathaes, G. Winter, A. Besheer, J. Engert, *Int. J. Pharm.* **2014**, *465*, 159.
- [143] M. Bartneck, H. A. Keul, S. Singh, K. Czaja, J. Bornemann, M. Bockstaller, M. Moeller, G. Zwadlo-Klarwasser, J. Groll, *ACS Nano* **2010**, *4*, 3073.
- [144] H. Herd, N. Daum, A. T. Jones, H. Huwer, H. Ghandehari, C. M. Lehr, *ACS Nano* **2013**, *7*, 1961.
- [145] Y. Geng, P. Dalhaimer, S. Cai, R. Tsai, M. Tewari, T. Minko, D. E. Discher, *Nat. Nanotechnol.* **2007**, *2*, 249.
- [146] Y. Geng, P. Dalhaimer, S. S. Cai, R. Tsai, M. Tewari, T. Minko, D. E. Discher, *Nat. Nanotechnol.* **2007**, *2*, 249.
- [147] X. Huang, L. Li, T. Liu, N. Hao, H. Liu, D. Chen, F. Tang, *ACS Nano* **2011**, *5*, 5390.
- [148] Z. Li, C. Xiao, T. Y. Yong, Z. F. Li, L. Gan, X. L. Yang, *Chem. Soc. Rev.* **2020**, *49*, 2273.
- [149] D. Guo, G. Xie, J. Luo, *J. Phys. D: Appl. Phys.* **2014**, *47*, 013001.
- [150] Y. Hui, X. Yi, F. Hou, D. Wibowo, F. Zhang, D. Zhao, H. Gao, C.-X. Zhao, *ACS Nano* **2019**, *13*, 7410.
- [151] A. C. Anselmo, M. Zhang, S. Kumar, D. R. Vogus, S. Menegatti, M. E. Helgeson, S. Mitragotri, *ACS Nano* **2015**, *9*, 3169.
- [152] J. Sun, L. Zhang, J. Wang, Q. Feng, D. Liu, Q. Yin, D. Xu, Y. Wei, B. Ding, X. Shi, X. Jiang, *Adv. Mater.* **2015**, *27*, 1402.
- [153] Z. G. Teng, C. Y. Wang, Y. X. Tang, W. Li, L. Bao, X. H. Zhang, X. D. Su, F. Zhang, J. J. Zhang, S. J. Wang, D. Y. Zhao, G. M. Lu, *J. Am. Chem. Soc.* **2018**, *140*, 1385.
- [154] Z. Shen, H. Ye, X. Yi, Y. Li, *ACS Nano* **2018**, *13*, 215.
- [155] P. Guo, D. Liu, K. Subramanyam, B. Wang, J. Yang, J. Huang, D. T. Auguste, M. A. Moses, *Nat. Commun.* **2018**, *9*, 130.
- [156] Y. Hui, D. Wibowo, Y. Liu, R. Ran, H.-F. Wang, A. Seth, A. P. J. Middelberg, C.-X. Zhao, *ACS Nano* **2018**, *12*, 2846.
- [157] M. B. Fish, C. A. Fromen, G. Lopez-Cazares, A. W. Golinski, T. F. Scott, R. Adili, M. Holinstat, O. Eniola-Adefeso, *Biomaterials* **2017**, *124*, 169.
- [158] K. Muller, D. A. Fedosov, G. Gompper, *Med. Eng. Phys.* **2016**, *38*, 2.
- [159] M. Cooley, A. Sarode, M. Hoore, D. A. Fedosov, S. Mitragotri, A. Sen Gupta, *Nanoscale* **2018**, *10*, 15350.
- [160] A. Kumar, R. G. H. Rivera, M. D. Graham, *J. Fluid Mech.* **2014**, *738*, 423.
- [161] A. Kumar, M. D. Graham, *Soft Matter* **2012**, *8*, 10536.
- [162] E. Carboni, K. Tschudi, J. Nam, X. L. Lu, A. W. K. Ma, *AAPS PharmSciTech* **2014**, *15*, 762.
- [163] H. L. Ye, Z. Q. Shen, Y. Li, *Soft Matter* **2018**, *14*, 7401.
- [164] C. Fornaguera, C. Solans, *Pharm. Nanotechnol.* **2018**, *6*, 147.
- [165] G. Sanita, B. Carrese, A. Lamberti, *Front. Mol. Biosci.* **2020**, *7*, 587012.
- [166] J. D. Friedl, V. Nele, G. De Rosa, A. Bernkop-Schnurch, *Adv. Funct. Mater.* **2021**, *31*, 2103347.
- [167] C. D. Walkey, J. B. Olsen, F. Y. Song, R. Liu, H. B. Guo, D. W. H. Olsen, Y. Cohen, A. Emili, W. C. W. Chan, *ACS Nano* **2014**, *8*, 2439.
- [168] M. N. Hossen, L. Wang, H. R. Chinthalapally, J. D. Robertson, K. M. Fung, S. Wilhelm, M. Bieniasz, R. Bhattacharya, P. Mukherjee, *Sci. Adv.* **2020**, *6*, eaba5379.
- [169] J. C. Lee, N. D. Donahue, A. S. Mao, A. Karim, M. Komarneni, E. E. Thomas, E. R. Francek, W. Yang, S. Wilhelm, *ACS Appl. Nano Mater.* **2020**, *3*, 2421.
- [170] L. Kou, J. Sun, Y. Zhai, Z. He, *Asian J. Pharm. Sci.* **2013**, *8*, 1.
- [171] T. S. Levchenko, R. Rammohan, A. N. Lukyanov, K. R. Whiteman, V. P. Torchilin, *Int. J. Pharm.* **2002**, *240*, 95.
- [172] S. G. Elci, Y. Jiang, B. Yan, S. T. Kim, K. Saha, D. F. Moyano, G. Y. Tonga, L. C. Jackson, V. M. Rotello, R. W. Vachet, *ACS Nano* **2016**, *10*, 5536.
- [173] G. Sahay, D. Y. Alakhova, A. V. Kabanov, *J. Controlled Release* **2010**, *145*, 182.
- [174] L. W. Shi, J. Q. Zhang, M. Zhao, S. K. Tang, X. Cheng, W. Y. Zhang, W. H. Li, X. Y. Liu, H. S. Peng, Q. Wang, *Nanoscale* **2021**, *13*, 10748.
- [175] B. Pelaz, P. d. Pino, P. Maffre, R. Hartmann, M. Gallego, S. Rivera-Fernández, J. M. de la Fuente, G. U. Nienhaus, W. J. Parak, *ACS Nano* **2015**, *9*, 6996.
- [176] N. B. Shah, G. M. Vercellotti, J. G. White, A. Fegan, C. R. Wagner, J. C. Bischof, *Mol. Pharmaceutics* **2012**, *9*, 2146.
- [177] Q. Dai, C. Walkey, W. C. W. Chan, *Angew. Chem. Int. Ed.* **2014**, *53*, 5093.
- [178] J. C. Y. Kah, K. Y. Wong, K. G. Neoh, J. H. Song, J. W. P. Fu, S. Mhaisalkar, M. Olivo, C. J. R. Sheppard, *J. Drug Targeting* **2009**, *17*, 181.
- [179] P. Mishra, B. Nayak, R. K. Dey, *Asian J. Pharm. Sci.* **2016**, *11*, 337.
- [180] S. Zalba, T. L. M. ten Hagen, C. Burgui, M. J. Garrido, *J. Controlled Release* **2022**, *351*, 22.
- [181] P. Grenier, I. M. d. O. Viana, E. M. Lima, N. Bertrand, *J. Controlled Release* **2018**, *287*, 121.
- [182] G. T. Kozma, T. Shimizu, T. Ishida, J. Szebeni, *Adv. Drug Delivery Rev.* **2020**, *154*, 163.
- [183] Q. Yang, T. M. Jacobs, J. D. McCallen, D. T. Moore, J. T. Huckaby, J. N. Edelstein, S. K. Lai, *Anal. Chem.* **2016**, *88*, 11804.
- [184] G. Storm, S. O. Belliot, T. Daemen, D. D. Lasic, *Adv. Drug Delivery Rev.* **1995**, *17*, 31.

- [185] S. S. Nogueira, A. Schlegel, K. Maxeiner, B. Weber, M. Barz, M. A. Schroer, C. E. Blanchet, D. I. Svergun, S. Ramishetti, D. Peer, P. Langguth, U. Sahin, H. Haas, *ACS Appl. Nano Mater.* **2020**, *3*, 10634.
- [186] W. Yang, L. Wang, M. Fang, V. Sheth, Y. Zhang, A. M. Holden, N. D. Donahue, D. E. Green, A. N. Frickenstein, E. M. Mettenbrink, T. A. Schwemley, E. R. Francek, M. Haddad, M. N. Hossen, S. Mukherjee, S. Wu, P. L. DeAngelis, S. Wilhelm, *Nano Lett.* **2022**, *22*, 2103.
- [187] W. Yang, A. N. Frickenstein, V. Sheth, A. Holden, E. M. Mettenbrink, L. Wang, A. A. Woodward, B. S. Joo, S. K. Butterfield, N. D. Donahue, D. E. Green, A. G. Thomas, T. Harcourt, H. Young, M. L. Tang, Z. A. Malik, R. G. Harrison, P. Mukherjee, P. L. DeAngelis, S. Wilhelm, *Nano Lett.* **2022**, *22*, 7119.
- [188] M. Debayle, E. Balloul, F. Dembele, X. Xu, M. Hanafi, F. Ribot, C. Monzel, M. Coppey, A. Fragola, M. Dahan, T. Pons, N. Lequeux, *Bio-materials* **2019**, *219*, 119357.
- [189] R. Tatumi, H. Fujihara, *Chem. Commun.* **2005**, 83.
- [190] F. Dembele, M. Tasso, L. Trapiella-Alfonso, X. Xu, M. Hanafi, N. Lequeux, T. Pons, *ACS Appl. Mater. Interfaces* **2017**, *9*, 18161.
- [191] B. R. Knowles, P. Wagner, S. Maclaughlin, M. J. Higgins, P. J. Molino, *ACS Appl. Mater. Interfaces* **2017**, *9*, 18584.
- [192] K. P. García, K. Zarschler, L. Barbaro, J. A. Barreto, W. O'Malley, L. Spiccia, H. Stephan, B. Graham, *Small* **2014**, *10*, 2516.
- [193] Z. G. Estephan, J. A. Jaber, J. B. Schlenoff, *Langmuir* **2010**, *26*, 16884.
- [194] R. R. Arviso, O. R. Miranda, D. F. Moyano, C. A. Walden, K. Giri, R. Bhattacharya, J. D. Robertson, V. M. Rotello, J. M. Reid, P. Mukherjee, *PLoS One* **2011**, *6*, e24374.
- [195] A. S. Pitek, S. A. Jameson, F. A. Veliz, S. Shukla, N. F. Steinmetz, *Biomaterials* **2016**, *89*, 89.
- [196] P. L. Rodriguez, T. Harada, D. A. Christian, D. A. Pantano, R. K. Tsai, D. E. Discher, *Science* **2013**, *339*, 971.
- [197] Y. Qie, H. Yuan, C. A. von Roemeling, Y. Chen, X. Liu, K. D. Shih, J. A. Knight, H. W. Tun, R. E. Wharen, W. Jiang, B. Y. S. Kim, *Sci. Rep.* **2016**, *6*, 26269.
- [198] N. M. Gulati, P. L. Stewart, N. F. Steinmetz, *Mol. Pharmaceutics* **2018**, *15*, 2900.
- [199] H. Li, K. Jin, M. Luo, X. Wang, X. Zhu, X. Liu, T. Jiang, Q. Zhang, S. Wang, Z. Pang, *Cells* **2019**, *8*, 881.
- [200] Y. Q. Wang, C. Huang, P. J. Ye, J. R. Long, C. H. Xu, Y. Liu, X. L. Ling, S. Y. Lv, D. X. He, H. Wei, C. Y. Yu, *J. Controlled Release* **2022**, *347*, 400.
- [201] Z. Wang, E. D. Hood, J. Nong, J. Ding, O. A. Marcos-Contreras, P. M. Glassman, K. M. Rubey, M. Zaleski, C. L. Espy, D. Gullipali, T. Miwa, V. R. Muzykantov, W. C. Song, J. W. Myerson, J. S. Brenner, *Adv. Mater.* **2022**, *34*, 2107070.
- [202] L. Wang, S. Wilhelm, *Nat. Mater.* **2023**, *22*, 282.
- [203] D. E. Tylawsky, H. Kiguchi, J. Vaynshteyn, J. Gerwin, J. K. Shah, T. Islam, J. A. Boyer, D. R. Boue, M. Snuderl, M. B. Greenblatt, Y. Shamay, G. P. Raju, D. A. Heller, *Nat. Mater.* **2023**, *22*, 391.
- [204] D. Lombardo, M. A. Kiselev, M. T. Caccamo, *J. Nanomater.* **2019**, *2019*, 3702518.
- [205] A. Angelova, V. M. Garamus, B. Angelov, Z. F. Tian, Y. W. Li, A. H. Zou, *Adv. Colloid Interface Sci.* **2017**, *249*, 331.
- [206] A. Angelova, B. Angelov, R. Mutafchieva, S. Lesieur, *J. Inorg. Organomet. Polym. Mater.* **2015**, *25*, 214.
- [207] S. Takano, Y. Aramaki, S. Tsuchiya, *Pharm. Res.* **2003**, *20*, 962.
- [208] S. A. Dilliard, Q. Cheng, D. J. Siegwart, *Proc. Natl. Acad. Sci. USA* **2021**, *118*, 2109256118.
- [209] R. Gref, M. Luck, P. Quellec, M. Marchand, E. Dellacherie, S. Harnisch, T. Blunk, R. H. Muller, *Colloids Surf., B* **2000**, *18*, 301.
- [210] J. L. Weaver, G. A. Tobin, T. Ingle, S. Bancos, D. Stevens, R. Rouse, K. E. Howard, D. Goodwin, A. Knapton, X. Li, K. Shea, S. Stewart, L. Xu, P. L. Goering, Q. Zhang, P. C. Howard, J. Collins, S. Khan, K. Sung, K. M. Tyner, *Part. Fibre Toxicol.* **2017**, *14*, 25.
- [211] T. Liu, H. Choi, R. Zhou, I. W. Chen, *Nano Today* **2015**, *10*, 11.
- [212] M. Germain, L. Poul, J. Devalliere, M. Paolini, A. Darmon, M. Bergere, O. Jibault, F. I. Mpambani, *Cancer Res.* **2019**, *79*, 3613.
- [213] M. R. A. Abdollah, T. Kalber, B. Tolner, P. Southern, J. C. Bear, M. Robson, R. B. Pedley, I. P. Parkin, Q. A. Pankhurst, P. Mulholland, K. Chester, *Faraday Discuss.* **2014**, *175*, 41.
- [214] R. L. Souhami, H. M. Patel, B. E. Ryman, *Biochim. Biophys. Acta* **1981**, *674*, 354.
- [215] M. R. A. Abdollah, T. J. Carter, C. Jones, T. L. Kalber, V. Rajkumar, B. Tolner, C. Gruettner, M. Zaw-Thin, J. B. Torres, M. Ellis, M. Robson, R. B. Pedley, P. Mulholland, R. T. M. de Rosales, K. A. Chester, *ACS Nano* **2018**, *12*, 1156.
- [216] I. B. Magana, R. B. Yendluri, P. Adhikari, G. P. Goodrich, J. A. Schwartz, E. A. Sherer, D. P. O'Neal, *Ther. Delivery* **2015**, *6*, 777.
- [217] L. Liu, T. K. Hitchens, Q. Ye, Y. J. Wu, B. Barbe, D. E. Prior, W. F. Li, F. C. Yeh, L. M. Foley, D. J. Bain, C. Ho, *Biochim. Biophys. Acta* **2013**, *1830*, 3447.
- [218] M. P. Nikitin, I. V. Zelepukin, V. O. Shipunova, I. L. Sokolov, S. M. Deyev, P. I. Nikitin, *Nat. Biomed. Eng.* **2020**, *4*, 717.
- [219] R. Palomba, M. di Francesco, V. di Francesco, F. Piccardi, T. Catelani, M. Ferreira, A. L. Palange, P. Decuzzi, *Mater. Horiz.* **2021**, *8*, 2726.
- [220] B. Vollmar, D. Rüttinger, G. A. Wanner, R. Leiderer, M. D. Menger, *Shock* **1996**, *6*, 434.
- [221] E. Huszti, G. Lázár, A. Párducz, *Br. J. Exp. Pathol.* **1980**, *61*, 624.
- [222] P. Cai, B. S. Kaphalia, G. A. S. Ansari, *Toxicology* **2005**, *210*, 197.
- [223] J. Wolfram, S. Nizzero, H. Liu, F. Li, G. Zhang, Z. Li, H. Shen, E. Blanco, M. Ferrari, *Sci. Rep.* **2017**, *7*, 13738.
- [224] P. Diagaradjane, A. Deorukhkar, J. G. Gelovani, D. M. Maru, S. Krishnan, *ACS Nano* **2010**, *4*, 4131.
- [225] M. Port, J. M. Idee, C. Medina, C. Robic, M. Sabatou, C. Corot, *BioMetals* **2008**, *21*, 469.
- [226] N. v. Rooijen, *J. Drug Targeting* **2008**, *16*, 529.
- [227] N. V. Rooijen, A. Sanders, *J. Immunol. Methods* **1994**, *174*, 83.
- [228] J. Hao, T. Han, M. Wang, Q. Zhuang, X. Wang, J. Liu, Y. Wang, H. Tang, *Drug Delivery* **2018**, *25*, 1289.
- [229] A. J. Tavares, W. Poon, Y. N. Zhang, Q. Dai, R. Besla, D. Ding, B. Ouyang, A. Li, J. Chen, G. Zheng, C. Robbins, W. C. W. Chan, *Proc. Natl. Acad. Sci. USA* **2017**, *114*, E10871.
- [230] Y. Ohara, T. Oda, K. Yamada, S. Hashimoto, Y. Akashi, R. Miyamoto, A. Kobayashi, K. Fukunaga, R. Sasaki, N. Ohkohchi, *Int. J. Cancer* **2012**, *131*, 2402.
- [231] Q. Hu, N. v. Rooijen, D. Liu, *J. Liposome Res.* **2008**, *6*, 681.
- [232] N. van Rooijen, E. Hendriks, *Methods Mol. Biol.* **2010**, *605*, 189.
- [233] Z. Z. Li, X. Xu, X. M. Feng, P. M. Murphy, *Sci. Rep.* **2016**, *6*, 22143.
- [234] N. VanRooijen, A. Sanders, *Hepatology* **1996**, *23*, 1239.
- [235] A. L. B. Seynhaeve, M. Amin, D. Haemmerich, G. C. van Rhooen, T. L. M. ten Hagen, *Adv. Drug Delivery Rev.* **2020**, *163*, 125.
- [236] A. M. Syed, S. Sindhvani, W. C. W. Chan, *Nat. Biomed. Eng.* **2017**, *1*, 629.
- [237] S. P. Li, Y. L. Zhang, J. Wang, Y. Zhao, T. J. Ji, X. Zhao, Y. P. Ding, X. Z. Zhao, R. F. Zhao, F. Li, X. Yang, S. L. Liu, Z. F. Liu, J. H. Lai, A. K. Whittaker, G. J. Anderson, J. Y. Wei, G. J. Nie, *Nat. Biomed. Eng.* **2017**, *1*, 667.
- [238] H. Meng, Y. Zhao, J. Y. Dong, M. Xue, Y. S. Lin, Z. X. Ji, W. X. Mai, H. Y. Zhang, C. H. Chang, C. J. Brinker, J. I. Zink, A. E. Nel, *ACS Nano* **2013**, *7*, 10048.
- [239] W. Jiang, Y. H. Huang, Y. An, B. Y. S. Kim, *ACS Nano* **2015**, *9*, 8689.
- [240] T. Meszaros, A. I. Csincsai, B. Uzonyi, M. Hebecker, T. G. Fulop, A. Erdei, J. Szebeni, M. Jozsi, *Nanomed. Nanotechnol.* **2016**, *12*, 1023.
- [241] Z. C. Wang, J. S. Brenner, *AAPS J.* **2021**, *23*.
- [242] H. Gaikwad, Y. Li, G. Gifford, E. Groman, N. K. Banda, L. Saba, R. Scheinman, G. K. Wang, D. Simberg, *Bioconjugate Chem.* **2020**, *31*, 1844.

- [243] G. Gifford, V. P. Vu, N. K. Banda, V. M. Holers, G. K. Wang, E. V. Groman, D. Backos, R. Scheinman, S. M. Moghimi, D. Simberg, *J. Controlled Release* **2019**, *302*, 181.
- [244] J. Gabrielsson, D. Weiner, *Methods Mol. Biol.* **2012**, *929*, 377.
- [245] S. M. Narum, T. Le, D. P. Le, J. C. Lee, N. D. Donahue, W. Yang, S. Wilhelm, in *Nanoparticles for Biomedical Applications*, (Eds: E. J. Chung, L. L. Carlos Rinaldi), Elsevier, Amsterdam **2020**, pp. 37–53.
- [246] T. D. T. Nguyen, R. Marasini, S. Rayamajhi, C. Aparicio, D. Biller, S. Aryal, *Nanoscale* **2020**, *12*, 4137.
- [247] U. Jakobsson, E. Makila, A. Rahikkala, S. Imlimthan, J. Lampuoti, S. Ranjan, J. Heino, P. Jalkanen, U. Koster, K. Mizohata, H. A. Santos, J. Salonen, A. J. Airaksinen, M. Sarparanta, K. Helariutta, *Nucl. Med. Biol.* **2020**, *84–85*, 102.
- [248] S. M. Gheibihayat, M. R. Jaafari, M. Hatamipour, A. Sahebkar, *J. Pharm. Pharmacol.* **2021**, *73*, 169.
- [249] J. Park, J. E. Park, V. E. Hedrick, K. V. Wood, C. Bonham, W. Lee, Y. Yeo, *Small* **2018**, *14*, 1703670.
- [250] J. Wang, R. Bai, R. Yang, J. Liu, J. L. Tang, Y. Liu, J. Y. Li, Z. F. Chai, C. Y. Chen, *Metallicomics* **2015**, *7*, 516.
- [251] T. Skotland, T. G. Iversen, A. Llorente, K. Sandvig, *Adv. Drug Delivery Rev.* **2022**, *186*, 114326.
- [252] O. S. Thomas, W. Weber, *Front. Bioeng. Biotechnol.* **2019**, *7*, 415.
- [253] V. Sheth, X. X. Chen, E. M. Mettenbrink, W. Yang, M. A. Jones, M'. O. Saad, A. G. Thomas, R. S. Newport, E. Francek, L. Wang, A. N. Frickenstein, N. D. Donahue, A. Holden, N. F. Mjema, D. E. Green, P. L. DeAngelis, J. Bewersdorf, S. Wilhelm, *ACS Nano* **2023**, *17*, 8376.
- [254] S. Sindhvani, A. M. Syed, S. Wilhelm, W. C. W. Chan, *Bioconjugate Chem.* **2017**, *28*, 253.
- [255] A. M. Syed, P. MacMillan, J. Ngai, S. Wilhelm, S. Sindhvani, B. R. Kingston, J. L. Y. Wu, P. Llano-Suarez, Z. P. Lin, B. Ouyang, Z. Kahiel, S. Gadde, W. C. W. Chan, *Nano Lett.* **2020**, *20*, 1362.
- [256] B. R. Kingston, Z. P. Lin, B. Ouyang, P. MacMillan, J. Ngai, A. M. Syed, S. Sindhvani, W. C. W. Chan, *ACS Nano* **2021**, *15*, 14080.
- [257] A. M. Syed, S. Sindhvani, S. Wilhelm, B. R. Kingston, D. S. W. Lee, J. L. Gommerman, W. C. W. Chan, *J. Am. Chem. Soc.* **2017**, *139*, 9961.
- [258] S. Sindhvani, A. M. Syed, S. Wilhelm, D. R. Glancy, Y. Y. Chen, M. Dobosz, W. C. W. Chan, *ACS Nano* **2016**, *10*, 5468.
- [259] M. Faria, M. Bjornmalm, K. J. Thurecht, S. J. Kent, R. G. Parton, M. Kavallaris, A. P. R. Johnston, J. J. Gooding, S. R. Corrie, B. J. Boyd, P. Thordarson, A. K. Whittaker, M. M. Stevens, C. A. Prestidge, C. J. H. Porter, W. J. Parak, T. P. Davis, E. J. Crampin, F. Caruso, *Nat. Nanotechnol.* **2018**, *13*, 777.
- [260] J. Lazarovits, S. Sindhvani, A. J. Tavares, Y. Zhang, F. Song, J. Audet, J. R. Krieger, A. M. Syed, B. Stordy, W. C. W. Chan, *ACS Nano* **2019**, *13*, 8023.
- [261] S. Zanganeh, R. Spitler, M. Erfanzadeh, A. M. Alkilany, M. Mahmoudi, *Int. J. Biochem. Cell Biol.* **2016**, *75*, 143.
- [262] Z. Ban, P. Yuan, F. Yu, T. Peng, Q. Zhou, X. Hu, *Proc. Natl. Acad. Sci. USA* **2020**, *117*, 10492.
- [263] R. García-Álvarez, M. Hadjidemetriou, A. Sánchez-Iglesias, L. M. Liz-Marzán, K. Kostarelos, *Nanoscale* **2018**, *10*, 1256.
- [264] C. Chen, Z. Yaari, E. Apfelbaum, P. Grodzinski, Y. Shamay, D. A. Heller, *Adv. Drug Delivery Rev.* **2022**, *183*, 114172.
- [265] X. Yan, A. Sedykh, W. Wang, B. Yan, H. Zhu, *Nat. Commun.* **2020**, *11*, 2519.
- [266] N. Serov, V. Vinogradov, *Adv. Drug Delivery Rev.* **2022**, *184*, 114194.
- [267] Z. M. Lin, W. C. Chou, Y. H. Cheng, C. L. He, N. A. Monteiro-Riviere, J. E. Riviere, *Int. J. Nanomed.* **2022**, *17*, 1365.
- [268] W. C. Chou, Q. R. Chen, L. Yuan, Y. H. Cheng, C. L. He, N. A. Monteiro-Riviere, J. E. Riviere, Z. M. Lin, *J. Controlled Release* **2023**, *361*, 53.
- [269] D. Ho, P. Wang, T. Kee, *Nanoscale Horiz.* **2019**, *4*, 365.
- [270] K. P. Das, J. Chandra, *Front. Med. Technol.* **2023**, *4*, 1067144.
- [271] A. V. Singh, M. Varma, P. Laux, S. Choudhary, A. K. Datusalia, N. Gupta, A. Luch, A. Gandhi, P. Kulkarni, B. Nath, *Arch. Toxicol.* **2023**, *97*, 963.
- [272] H. C. Tao, T. Y. Wu, M. Aldeghi, T. C. Wu, A. Aspuru-Guzik, E. Kumacheva, *Nat. Rev. Mater.* **2021**, *6*, 701.
- [273] T. Lunnoo, J. Assawakhajornsak, T. Puangmali, *J. Phys. Chem. C* **2019**, *123*, 3801.
- [274] A. V. Singh, M. H. D. Ansari, D. Rosenkranz, R. S. Maharjan, F. L. Kriegel, K. Gandhi, A. Kanase, R. Singh, P. Laux, A. Luch, *Adv. Healthcare Mater.* **2020**, *9*, 1901862.
- [275] M. K. Jayasinghe, C. Y. Lee, T. T. T. Tran, R. Tan, S. M. Chew, B. Z. J. Yeo, W. X. Loh, M. Pirisinu, M. T. N. Le, *Front Digit Health* **2022**, *4*, 35.
- [276] X. L. Yan, A. Sedykh, W. Y. Wang, X. L. Zhao, B. Yan, H. Zhu, *Nanoscale* **2019**, *11*, 8352.
- [277] G. Yamankurt, E. J. Berns, A. Xue, A. Lee, N. Bagheri, M. Mrksich, C. A. Mirkin, *Nat. Biomed. Eng.* **2019**, *3*, 318.
- [278] V. Mittelheisser, P. Coliat, E. Moeglin, L. Goepf, J. G. Goetz, L. J. Charbonniere, X. Pivot, A. Detappe, *Adv. Mater.* **2022**, *34*, 2110305.
- [279] O. Abdifetah, K. Na-Bangchang, *Int. J. Nanomed.* **2019**, *14*, 5659.
- [280] F. Fan, B. Xie, L. H. Yang, *ACS Appl. Bio Mater.* **2021**, *4*, 7615.
- [281] L. S. L. Price, S. T. Stern, A. M. Deal, A. V. Kabanov, W. C. Zamboni, *Sci. Adv.* **2020**, *6*, eaay9249.
- [282] Y. H. Cheng, C. L. He, J. E. Riviere, N. A. Monteiro-Riviere, Z. M. Lin, *ACS Nano* **2020**, *14*, 3075.
- [283] H. I. Labouta, N. Asgarian, K. Rinker, D. T. Cramb, *ACS Nano* **2019**, *13*, 1583.



Lin Wang is a postdoctoral research fellow within Prof. Stefan Wilhelm's team at the Stephenson School of Biomedical Engineering, University of Oklahoma. Her research interests focus on understanding the nanomedicine-biological system interactions, as well as developing novel nanoparticle engineering strategies to improve nanomedicine delivery efficiency and therapeutic efficacy.



Skyler Quine graduated in 2020 with an M.S. in biomedical engineering from the University of Oklahoma. His passion for the scientific method and graphic design has led him on a path, including roles as a scientist, executive recruiter, DJ, videographer, head of marketing, and more. Today he lives in Austin with his loving wife, goofy dog, and fluffy cat. He spends his time advancing the careers of top pharma executives, leading marketing for a piano lesson startup, DJing weddings and events, rock climbing, and keeping Life guessing as to what he will do next.



Lucila Garcia-Contreras is an associate professor in the Department of Pharmaceutical Sciences at the Oklahoma University Health Sciences Center. She is particularly known for her work on the design and formulation of therapeutic compounds, pulmonary administration of compounds to laboratory animal models, and pharmacokinetics of inhaled drugs and tuberculosis. She has published several articles and book chapters in the pharmaceutical and biomedical literature on the delivery and disposition of drugs and vaccines after pulmonary administration as well as novel approaches to treat gynecological and lung cancers.



Yan D. Zhao is a presidential professor of biostatistics at the University of Oklahoma Health Sciences Center. He is the associate dean for research in the Hudson College of Public Health. He is also the associate director of biostatistics and research design Shared Resources at the Stephenson Cancer Center. His research areas include the design and analysis of clinical trials, nonparametrics, multiple testing, and adaptive design. He has published more than 120 refereed papers, and currently he is an associate editor for pharmaceutical statistics.



Stefan Wilhelm is an associate professor of biomedical engineering at the University of Oklahoma. He received the 2021 National Science Foundation CAREER award and was named a 2021 Scialog Fellow for Advancing Bioimaging by the Research Corporation for Science Advancement. In 2023, he received the R35 MIRA award from the National Institutes of Health. His research focuses on developing novel nanomedicines for cancer drug delivery, diagnostics, and vaccine applications.